MODEL STUDIES OF REINFORCED CONCRETE SKEW SLAB AND BEAM BRIDGES UNDER ULTIMATE LOADS

A THESIS

PRESENTED TO

THE FACULTY OF THE GRADUATE STUDIES AND RESEARCH

THE UNIVERSITY OF MANITOBA

IN PARTIAL FULFILMENT

OF THE REQUIREMENTS FOR THE DEGREE

MASTER OF SCIENCE

by

JENN - CHING YIH

MARCH 1967

ABSTRACT

The simply supported reinforced concrete slab and beam bridge for 2 - lane traffic with a skew angle of 30 degrees was analyzed by using purely plastic behaviour, yield lines and yield hinges, under H20-S16 highway truck loading.

Two $\frac{1}{6}$ - scale models were built in the laboratory for three tests:

(1). Four wheel loads were applied on one side of the bridge beams.

(2). Two wheel loads were applied on the slab.

(3). Four wheel loads were applied on two internal beams.

The test results show that the combined yield lines and yield hinges method is valid and safe for skew composite structures within certain limitations.

ACKNOWLEDGMENTS

The writer would like to express his thanks to his supervisor, Prof. A. M. Lansdown of the Civil Engineering Department, the University of Manitoba, for his guidance and assistance throughout this project.

Sincere thanks are extended to writer's collegues Mr. W. Dolhun for his reading and valuable suggestions, Mr. S. Teerachaichyuti and Y. Kang for their help in building the models.

To those in the materials laboratory, Messrs. E. Lemke, D. Drul, R. Muir and H. Brooks, the writer expresses his thanks for their assistance in building equipment, test models and in the actual testing.

LIST OF FIGURES

LIST OF FIGURES

LIST OF TABLES

LIST OF PHOTOGRAPHS

TABLE OF CONTENTS

CHAPTER I

INTRODUCTION

The rapid development of highway engineering makes the skew bridges important, especially for short or medium spans up to 60 feet. These are often built as overpasses or underpasses in the area where highways cross inclined brooks, rivers, drainage systems, railways or other highways. Hence, the design and research of skew bridges are becoming more urgent and interesting.

In the last thirty years vast research work about skew structures has been done on the basis of elastic theory. However, research work based on the plastic behavior is scarce.

One of earliest mathematical solution of the two sided simply supported skew slab under uniformly distributed load was given by Anzelius[a] in 1939. At the same time Vogt[b] calculated two- and four-sided simply supported slabs under uniformly distributed load with skew angles of 30- and 45-degrees and compared its moments with right slabs. Jensen[c] applied a finite difference procedure to a skew plate in 1941. Nielsen[d] (1944) investigated two sided simply supported slabs with a different skew angle and different side ratio under three loading conditions:

(a) Uniformly distributed load over the whole area.

(b) Concentrated load in the center of the skew plate.

(c) Concentrated load in the center of the free edge.

For practical purposes, the influence surface of four sided simply supported and four sided fixed slabs with 30° skew angle was developed by Graudenz[e] in 1948. The exact solution for deflections of parallelogram plates under uniformly distributed load was published by Fuchssteiner[f] (1953). Rüsch[g] (1956) estimated a rough approximation of moments for two sides simply supported plate with skew angle 15, 30, 45 and 60 degrees. Homberg and Marx[h] (1958) worked on two sided simply supported plate with different skew angle and a constant side ratio of one. Robinson[i] (1959) modified Jensen's approach to certain skew plates and tabulated the influence coefficients for the deflection at any mesh point due to concentrated load.

Other important parts of skew bridges are stiffened skew members and skew grillages. The former has been discussed by Homberg and Marx[h] and the latter were given by Beer and Resinger[j] in 1955 and Starke[k] in 1956 respectively.

The effect of skew on the behavior of I-Beam bridges having skew angles of 30 and 60 degrees was tested by Siess and Newmark[l] at the experimental station of the University of Illinois in 1948. The finite difference approach was also applied for solving composite skew bridges by Chen, Siess and Newmark[m] in 1957.

All above mentioned research works were based on elastic theory. Research works on the basis of plastic behavior are scattered. Some model tests of skew slab bridges with curbs under ultimate load with skew angles of 45 and 60 degrees were carried out in the laboratory of the University of Illinois by Grossard, Siess, Newmark and Goodman[(n)] in 1950. A research report from Granholm and Rowe[(o)] about skew slab was published in 1961. Also some textbooks[(p),(q)] have mentioned skew slabs under ultimate load. The plastic effect of torsion in the reinforced concrete beams and the method of combining of yield lines and yield hinges for composite structures were developed and discussed by Lansdown[(r)] in 1964.

This study is intended to analyze the skew slab and beam bridges by employing the method of combined yield lines and yield hinges and to compare with the test results of two $\frac{1}{6}$ scale models, on which three tests were carried out by the writer.

(1) Four wheel loads were applied on one side of the bridge beams

(2) Two wheel loads were applied on the slab.

(3) Four wheel loads were applied on two internal beams.

The model considered here is a simply supported skew bridge with an angle of 30 degrees, a normal span of 60 inches, and roadway clear width of 56 inches. The models were designed for two lane traffic and reduced H20-S16 highway loads.

1. Historical Bibliography

(a) Anzelius, A. (1939) — "Über die elastische Deformation parallelogrammförmiger Platten." Bauing. Bd. 20 (1939) S. 478.

(b) Vogt, H. (1939) — "Beitrag zur Berechnung schiefwinkliger Platten nebst Anwedung bei der Berechnung und Anordnung der Bewehrung schiefwinkliger Brückenbauwerke." Diss. T. H. Hannover 1939.

(c) Jensen, V. P. (1941) — "Analysis of skew slabs." University of Illinois. Bulletin Series No. 332 Vol. XXXIX. Sept. 1941, No. 3.

(d) Nielsen, N. J. (1944) — Reference of (h).

(e) Graudenz, H. (1948) — "Beitrag zur Berechnung der Momenten-Einflussfelder schiefwinkliger Platten." Diss. T. H. Hannover 1948.

(f) Fuchssteiner, W. (1953) — "Entwicklungsfunktion für polygonal begrenzte dünne Platten." Bauing. Bd. 28 (1953) S 243.

(g) Rüsch, H. (1956) "Fahrbehnplatten von Strassenbrücken." Deutscher Ausschuss fur stahlbeton, H 106. Berlin (1956)

(h) Homberg, H. and Marx, W. (1958) "Schief Stäbe und Platten." Werner Verlay, Dusseldorf, 1958, 324 pp.

(i) Robinson, K. E. (1959) "The behaviour of simply supported skew bridge slabs under concentrated loads." Cement and Concrete Association, London, Research Report No. B, Nov. 1959.

(j) Beer, H. and Resinger, F. (1955) "Genaue Berechnung Schiefer Trägerrostbrücken mit Einflusslinien." Bauing. Bd. 30 1955 S. 425

(k) Starke, J. J. (1956) "Beitrag Zur Berechnung schiefer Trägerroste." Stahlbau Bd. 25 (1956) S. 251.

(l) Siess, C. P. and Newmark N. M. (1948) "Studies of slab and beam highway bridges, Part II Tests of simple-span skew I-Beam bridges." The Eng. Exp. Sta. Uni. of Ill. Vol. 45, No. 31. Jan. 1948 Bull. No. 375

(m)	Chen, T. Y. Siess, C. P. Newmark, N. M. (1957)	"Studies in slab and beam highway bridges, Part VI. Moments in simply supported skew I-beam bridges." Uni. of Ill., Eng'g. exp. sta. Bull. 439, 1957, 72 pp.
(n)	Grossard, Siess, C. P. Newmark, N. M. Goodman (1950)	"Studies of highway skew slab-bridges with curbs. Part II. Laboratory Research." Eng. Exp. Sta. Uni. of Ill. Bull. No. 386. Vol. 47, No. 46. 1950.
(o)	Cranholm, C. and Rowe, R. E. (1961)	"The ultimate load of skew slab bridges." Cement and Concrete Association, London, Research Report. Rep. 12.
(p)	Rowe, R. G. (1962)	"Concrete Bridge Design. John Wiley & Sons, Inc. N. Y. 1962
(q)	Jones, L. L. (1962)	Ultimate Load Analysis of Reinforced and Prestressed Concrete Structures." Chatto & Windus Ltd. London, 1962. pp. 248.
(r)	Lansdown, A. M. (1964)	" An Investigation into the Ultimate Behaviour of Reinforced Concrete Beam and Slab Structures, in Particular Bridge Decks." Ph. D. Thesis, Uni. of Southampton. June 1964. pp. 146.

2. Definitions of terms

skew span ——————— the span parallel with the traffic lanes

normal span ——————— the span perpendicular to the abutments

skew angle ——————— the angle between the direction of the traffic lanes and a line perpendicular to the abutments

skew crossing —————— the angle between road axes

sagging yield line —— positive yield line

hogging yield line ———negative yield line

3. Notations

L ——— skew span

$\bar{l}$ ———— normal span

b ———— road width

m ———— plastic moment of slabs

M_B(.)—— bending moment of beams

M_T(o)———torsional moment of beams

⦿ —— combined bending and torsional hinge

P, ⊠ ———point load

〰〰 ———sagging line

--- ———hogging line

δ ——— deflection

θ ——— rotation of mechanism or beam

ψ ---- skew angle

ϕ ---- diameter of bars

A_s ---- steel area

f_y ---- yield stress of steel

$(d-\frac{a}{z})$ -- moment arm

K_ℓ ---- the proportional steel on the long side

K_s --- the proportional steel on the short side

Acage -- the cross section area enclosed by the reinforcement cage

$R_{min} = \frac{n\ FyL}{C}$ or $\frac{FyT}{P}$ whatever is lesser

n ---- numbers of longitudinal bars

F_{yL} --- yielding strength of one longitudinal bar

F_{yT} --- yielding force per unit length of beams

c ---- circumference of cage

p ---- pitch of the stirrups

P_u --- concentrated ultimate load

W_u --- uniformly distributed ultimate load

M --- plastic moment (bending or torsion)

ℓ'' --- length of yield line

CHAPTER 2

THE PROBLEM OF SKEW

In skew crossings, there are two types of bridges[1] that can be built. One is the right bridge (see Figure 1) which is of course more expensive but easier to analyze and construct. The other is the skew bridge

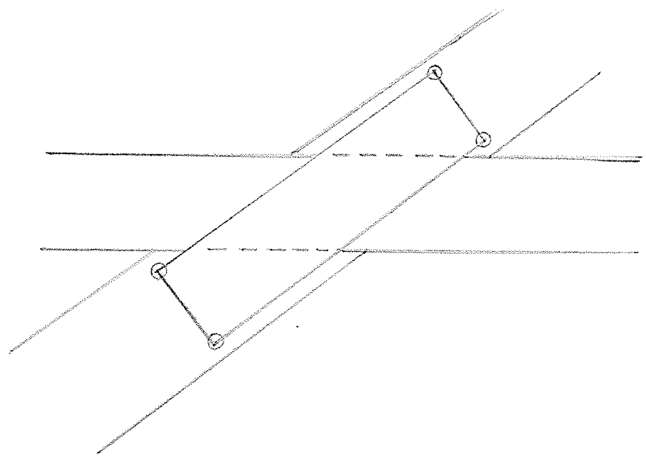

Figure 1

(see Figure 2) which is less expensive but more difficult to analyze and construct. The exact or approximate

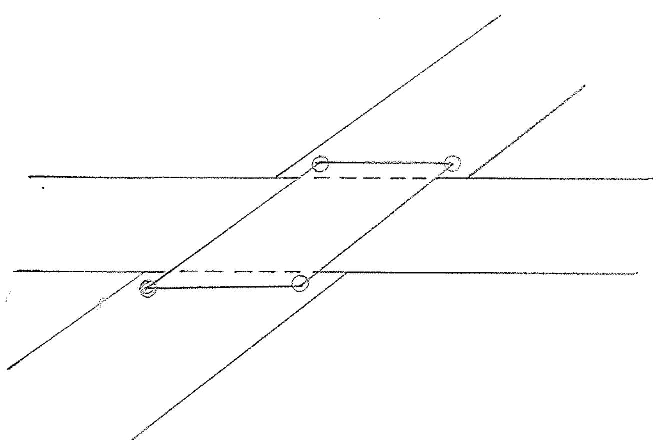

Figure 2

solution of skew slab and beam bridge is still not well developed. Studies of composite bridges[(2),(3)] from the University of Illinois show that the maximum moment in the I-beam decreases and the maximum moment in the middle of the slab increases. Hence, the effect of skew for slabs is more important than for beams. For this reason skew slabs are discussed herein both in elastic and plastic behaviour.

(1) <u>Elastic behaviour:</u>

The effect of skew depends on the skew angle and right width over normal span ratio.[(4)] For a small skew angle of less than 30 degrees with a right width over normal span ratio equal to or greater than 3, the slab can be treated as a right slab so long as the normal span line lies within the interval 0.8b as shown in Figure 3. If the normal span line lies outside the interval 0.8b, the distance between obtuse angles can be chosen as span length as shown in Figure 4.

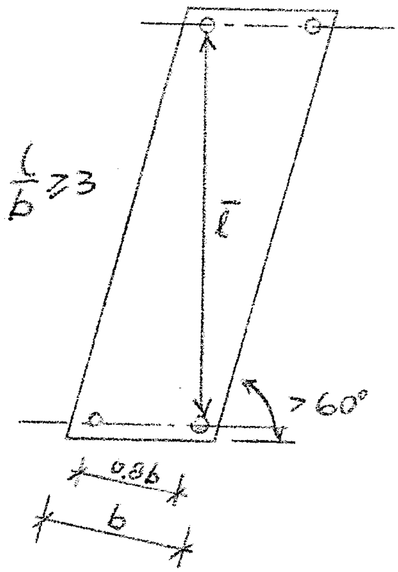

Figure 3

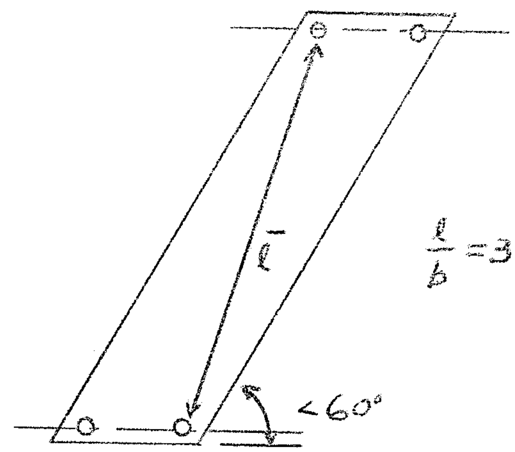

Figure 4

For a skew angle greater than 30 degrees the effect of skew is very pronounced, because the force would be transferred to the support by the shortest route which means a main carrying system formed from obtuse angle to obtuse angle as shown in Figure 5 by the crosshatched area.

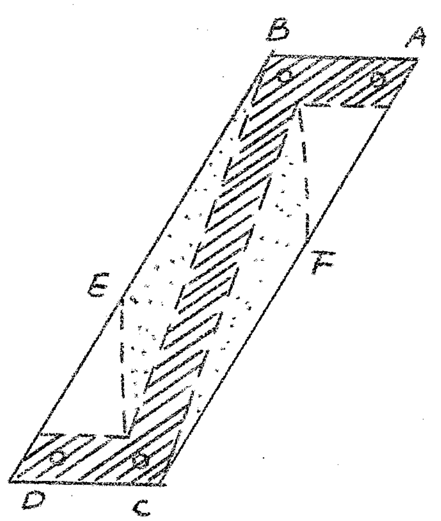

Figure 5

The dotted areas in Figure 5 are considered to concur with BC and two small triangles ABF and DCE act as the cantilevers AB and CD. When BC, the narrow strip, is loaded it will be found that the BC strip can not be rotated but is rigid at B and C. Its degree of rigidity depends on the skew angle. The larger the degree of skew the larger the rigidity should be. In this case the analysis of distribution of moments is rather laborious.

In certain cases, such as with the degree of skew of 0, 15, 30, 45, and 60 degrees and right width over normal span ratios of 2, 1.5, 1.0, 0.75 and 0.5 of isotropic plates, a comparatively simple mehtod is to use Robinsons's[5] tables of influence coefficients for deflection, and to substitute the deflections to its corresponding moment equations. For other cases Jensen's[5] finite difference procedure is available.

For composite skew bridges,[6] main girders are usually placed parallel to the direction of the road and the design span of the girders is measured along the same direction. For wide crossings with large skew angles the main girders may be placed perpendicular to the abutment, as shown in Figure 6. At each side of the crossing, the parapet girders carry the loads of the short beams.

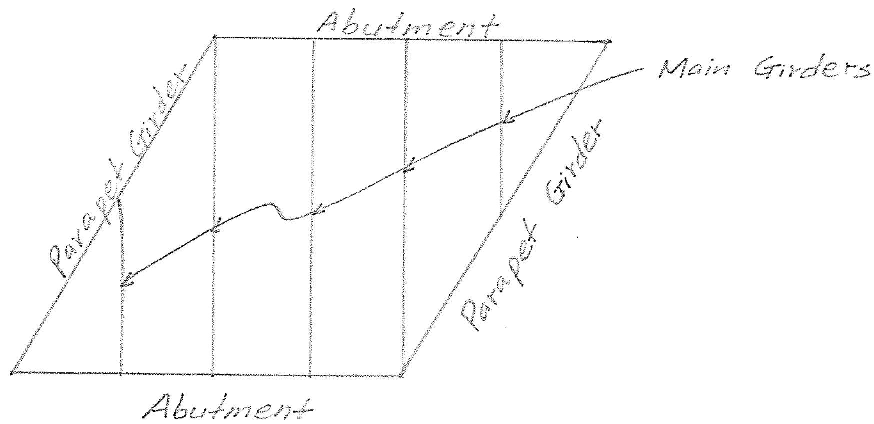

Figure 6

(2) Plastic behaviour:

Since the yield line pattern of skew slabs is similar to right slabs, the ultimate load analysis for skew slabs is rather simple. It can be considered that the skew slabs are the general case and the right slab is only a special case with an angle of skew equal to zero. A comparative number of examples were given by Jones.[7]

CHAPTER 3

BRIDGE ANALYSIS

(1) Description of prototype structure

The prototype structure considered in this study is a simply supported skew bridge with an angle of 30 degrees, a normal span of 30 feet, and roadway clear width of 28 feet. The bridge, which carries two lane traffic of H20-S16 highway truck loads, consists of a concrete slab with a uniform thickness of 12 inches and four uniformly spaced reinforced concrete beams of 2' x 4' in the direction of traffic and two transverse beams of 2.5' x 4' at each end of the bridge parallel to the abutment as shown in figure 7.

(2) Scale factor[9]

It is difficult and also not necessary to build a prototype structure for testing. Instead of that a small scale model is always built in the laboratory. The relationship of stress, strain, linear dimensions, steel areas and loads between prototype and model are demonstrated as follows:

Figure 7 -1

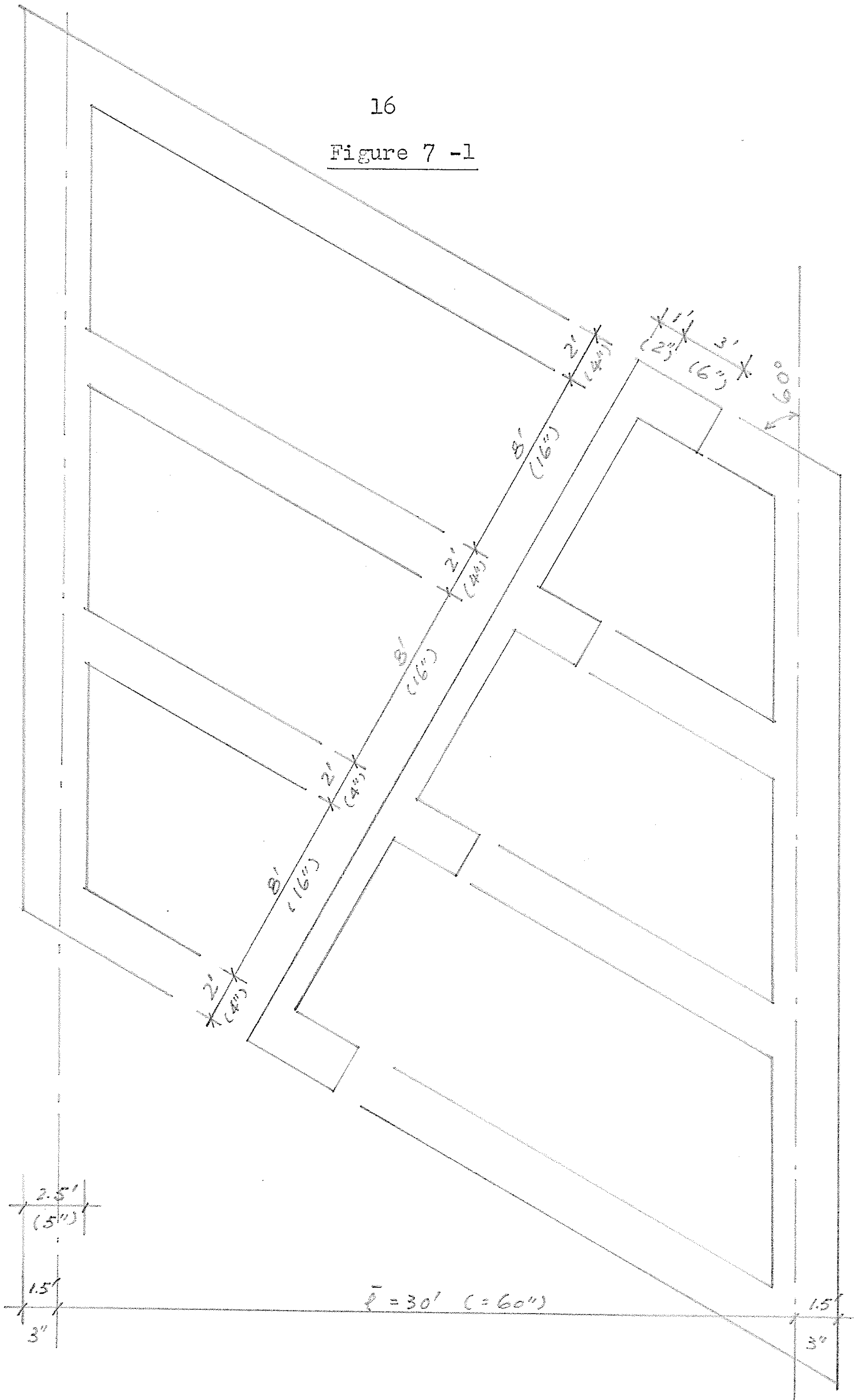

$$\alpha = \frac{f_p}{f_m}$$

α ------ stress scale

f_p ------ stress in prototype material

f_m ------ stress in model material

$$\beta = \frac{\varepsilon_p}{\varepsilon_m}$$

β ------ strain scale

ε_p ------ strain in prototype material

ε_m ------ strain in model material

$$\lambda = \frac{\ell_p}{\ell_m}$$

λ ------ linear scale

ℓ_p ------ dimension of prototype structure

ℓ_m ------ dimension of model structure

scale of steel areas $= \dfrac{\alpha \lambda^2}{\beta} = \dfrac{A_p}{A_m}$

A_p ------ Steel area in prototype structure

A_m ------ Steel area in model structure

scale of loads ---------- for uniform distributed load

$$W_m = \frac{W_p}{\alpha}$$

W_m ------ load per unit area to be applied to model

W_p ---- load per unit area acting on prototype structure for concentrated load.

P_m ---- concentrated load on model structure

P_p ---- concentrated load on prototype structure

$$P_m = Pp/\alpha\lambda^2$$

Accordingly, the dimensions and loads of prototype and model bridges are given in Table 1.

TABLE I

	Prototype	Model
Skew span (L)	35'	70''
Normal span ($\bar{\ell}$)	30'	60''
Road width (b)	28'	56''
Beam space	10'	20''
Beam section	2' x 4'	4'' x 8''
Truck load	24 (kips)	662#

(3) Design of model structure:

In order to comply with the AASHO[10] specifications two elastic bridge designs have been carried out. One was prototype design and the other was model design. For the purpose of this study the bridges have also been designed and investigated by using purely yield line theory.

(a) Prototype structure: The full-scale bridge was designed following AASHO specifications.

(b) Model design: The model was designed directly using reduced loads from the full scale loads according to the scale factor as discussed in the preceding paragraph.

(c) Ultimate load design: The ultimate load design of slabs is well established.(7),(11) But for a composite slab and beam system there are too many unknowns to be solved, if the yield lines and yield hinges are considered together with the assumed loads. For an example the bridge used in this study might have 10 unknowns in a virtual work equation as shown in figure 8. The equation can be written as

$$f(Wu,\ Pu) = f(m_1, m_2, m_3, m_4, M_B', M_B'', M_B''', M_T', M_T'', M_T''')$$

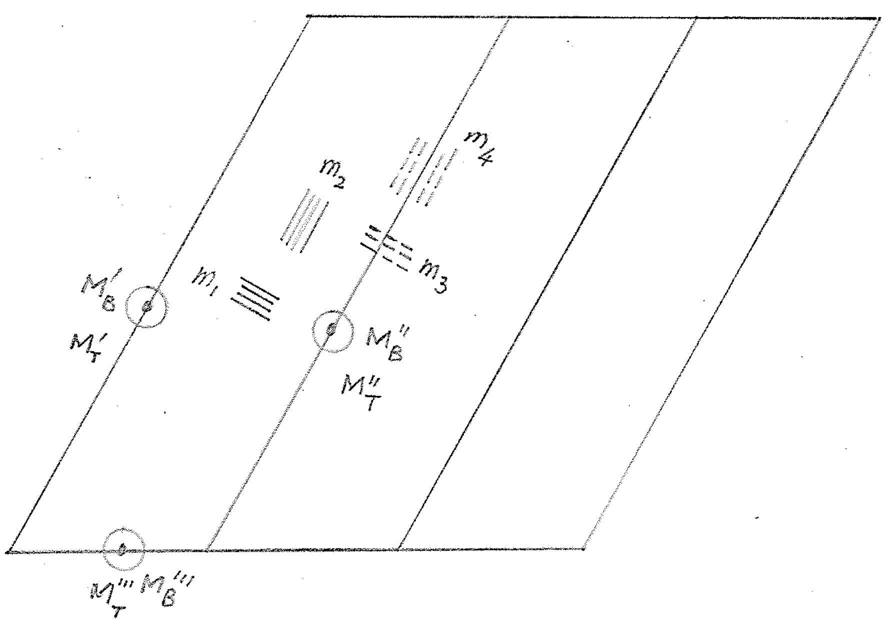

Figure 8

It can be simplified by assuming an isotropic deck and neglecting the bending moment in the transeversal beam and also assuming that the external and internal beams have the same bending and twisting moments.

Then the equation becomes

$$f\,(Wu,\ Pu) = f\,(m,\ M_B\ M_T\ M_T')\,.$$

Nevertheless, it is still impossible to solve directly

In order to make the ultimate load design of a composite structure possible, some suggestions are made.

(i) Assume the beams which surround the slabs strong enough, so the slab can be considered as fixed on four sides. Then draw the possible yield line family under the suggested loads, as shown in the following Figures 9, 10, 11 and 12.

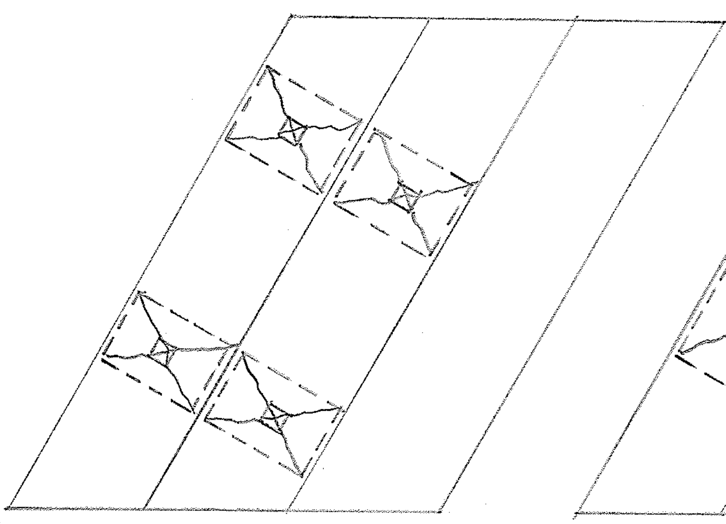

Figure 9

$Pu = 16m_1$

$m_1 = \frac{1}{16}\ Pu$

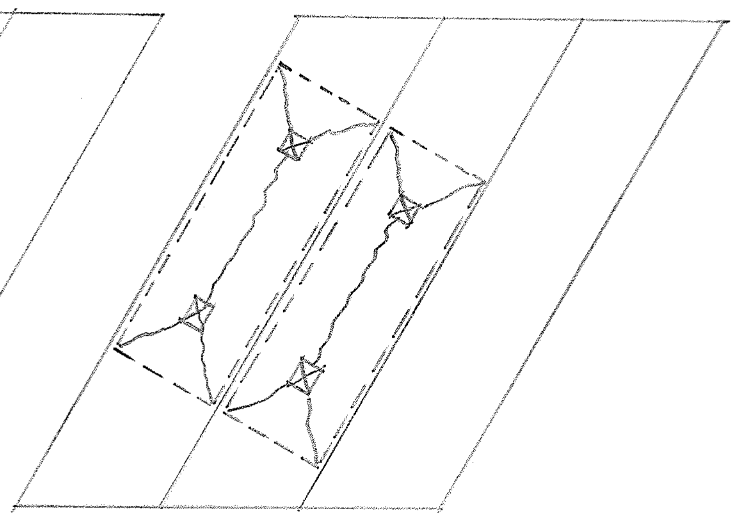

Figure 10

$Pu = 15m_2$

$m_2 = \frac{1}{15}\ Pu$

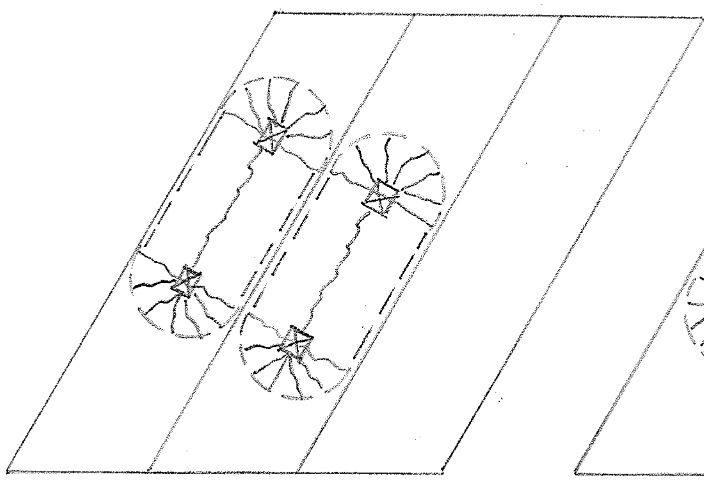

Figure 11

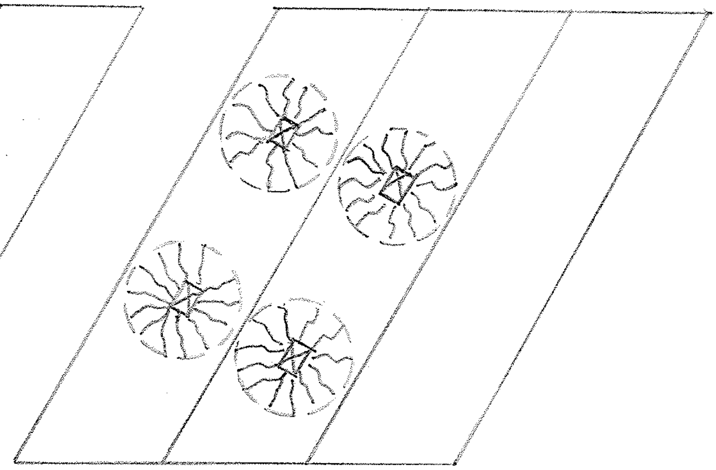

Figure 12

$Pu = 13.28\ m_3$

$$m_3 = \frac{1}{13.28} Pu$$

$Pu = 12.56\ m_4$

$$m_4 = \frac{1}{12.56} Pu$$

Here m_4 is the maximum value and controls the design of the slab. In the design, only the concentrated loads were considered.

(ii) To be on the safe side, in the beam design it can be assumed that the twisting strength of the beams are equal to zero and that the minimum moments in the slabs are taken into account, as shown in figure 13 and its virtual work equation.

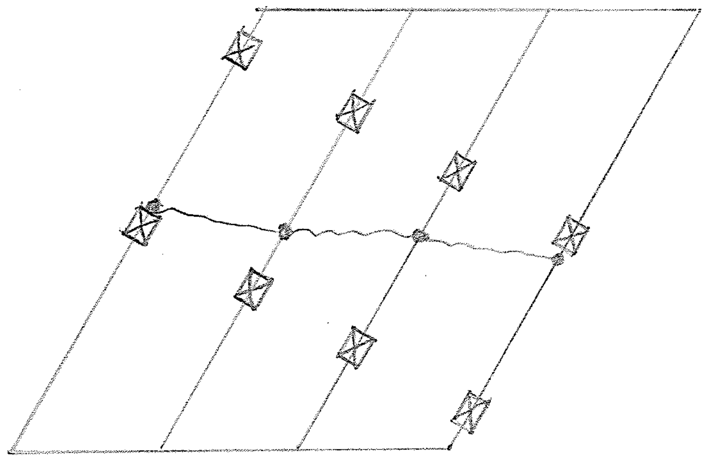

$$f(Pu) = f(m_{min}, \quad M_B, M_T, M_T)$$

Figure 13

(iii) When two ultimate concentrated truck loads act on the slab, the other possible yield patterns are shown in the Figures 14 and 15. To make the torsional and negative slab moments equal, the twisting moment of the external beam can be roughly estimated as $M_T = \frac{1}{2} \ell \cdot m_{max}$.

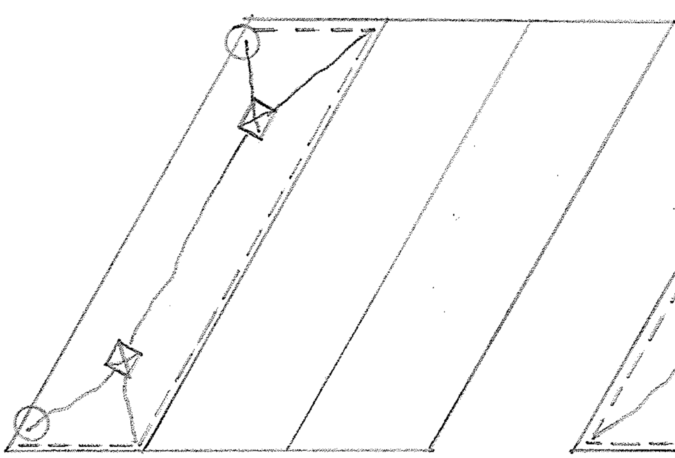

Figure 14

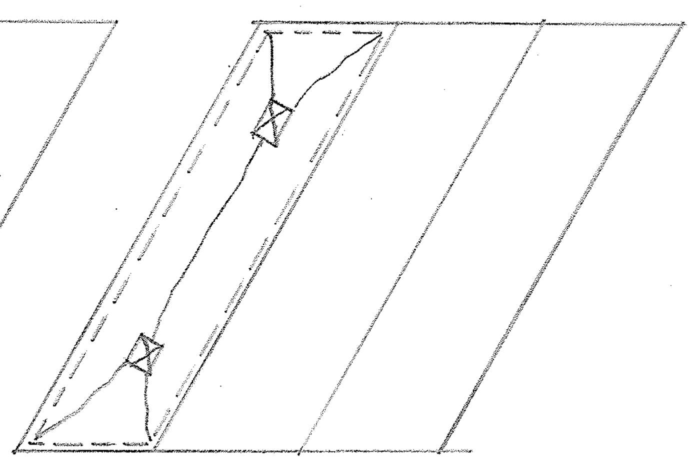

Figure 15

(d) Ultimate load investigation:[8] From the slab and beam details in the Appendix and the previous demonstrated bridges or other existing structures, we can calculate the ultimate moments of the sections and postulate the yield line patterns of the structure, upon which the minimum ultimate loads can be estimated. For the detailed calculations see Chapter 5.

CHAPTER 4

MODEL TESTS

(1) Construction of models:

Form work was built directly on the concrete floor in the laboratory. Two sheets of $\frac{1}{2}$" plywood were laid on the floor. The side forms of $\frac{3}{4}$" plywood were built on the $\frac{1}{2}$" plywood. For slabs $\frac{1}{4}$" plywood was used. All form work was connected by nails, as shown in Picture 1.

All reinforcing steel was cut to length and bent by laboratory personnel. The bars for the slabs and beams were tied together using standard ties. Slab bars were placed perpendicular to the direction of beams and were bent down along the outer faces of the external beams to form the anchorage both in top and bottom, while the bars parallel to the beams provided with standard hooks at each end. Stirrups were used both in the longitudinal and transversal beams at a 5" spacing. At the corner of the beams two extra $\frac{3}{16}$" ϕ bars were added as an anchorage. Eight lifting hooks were placed at the ends of the longitudinal beams, as shown in Pictures 2 and 3.

The concrete had a water / cement ratio of 0.507 and a maximum aggregate size of $\frac{3}{4}$" ϕ. High early strength cement was used for the concrete. After the concrete had been finished as shown in Picture 4 the complete structure was covered with wet burlap for at least 3 days. The first

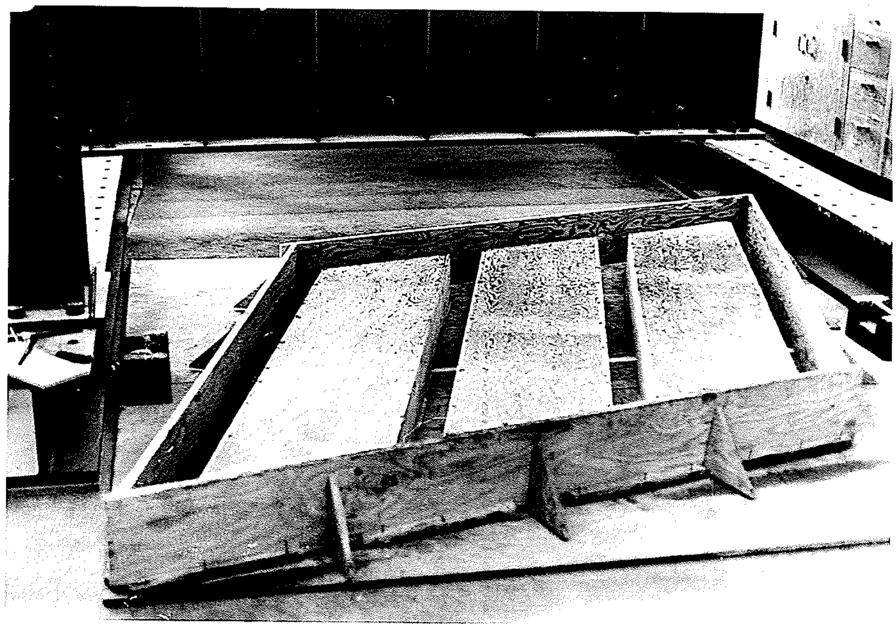

Picture 1

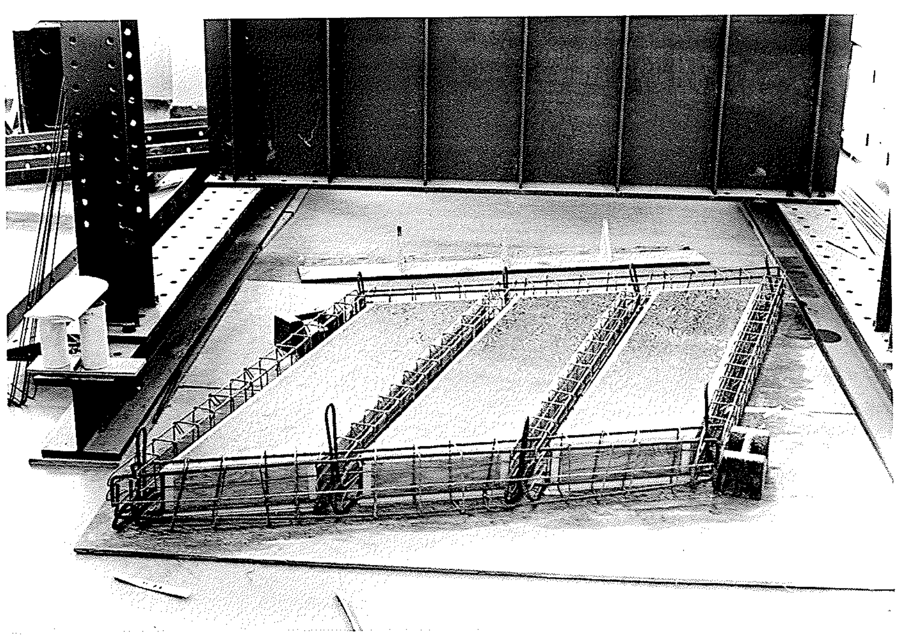

Picture 2

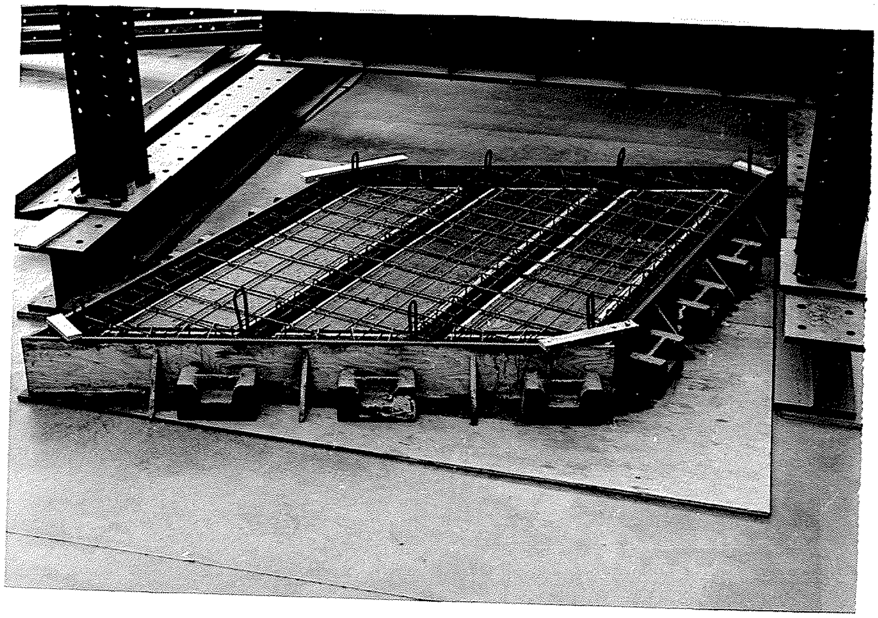

Picture 3

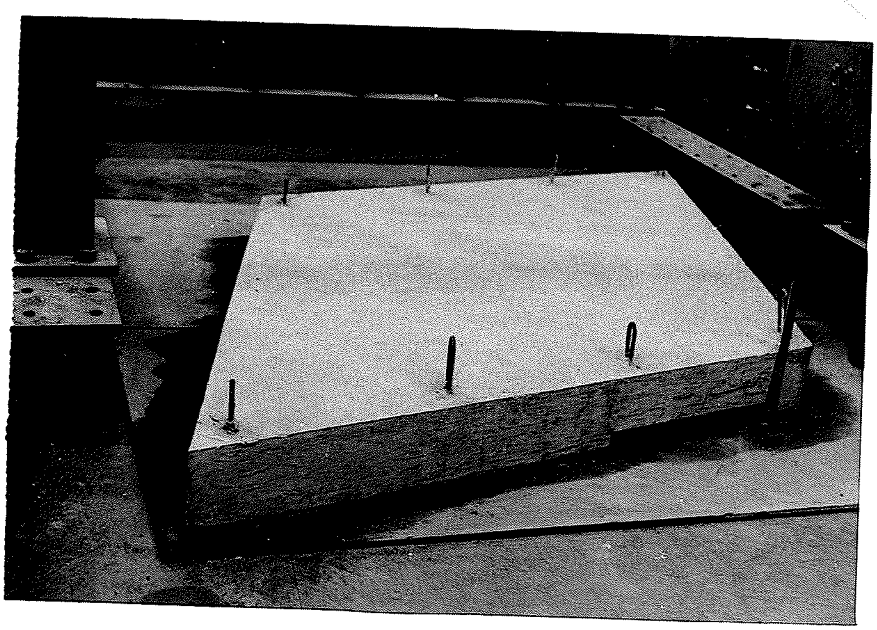

Picture 4

bridge was removed from the form after one week of curing and placed in position on the testing frame. It was supported by one fixed hinge, one one-direction movable support and six two-direction movable supports as shown in Picture 5 and Figure 16. Two wedged wood blocks were placed at each end of the bridge to increase the safety.

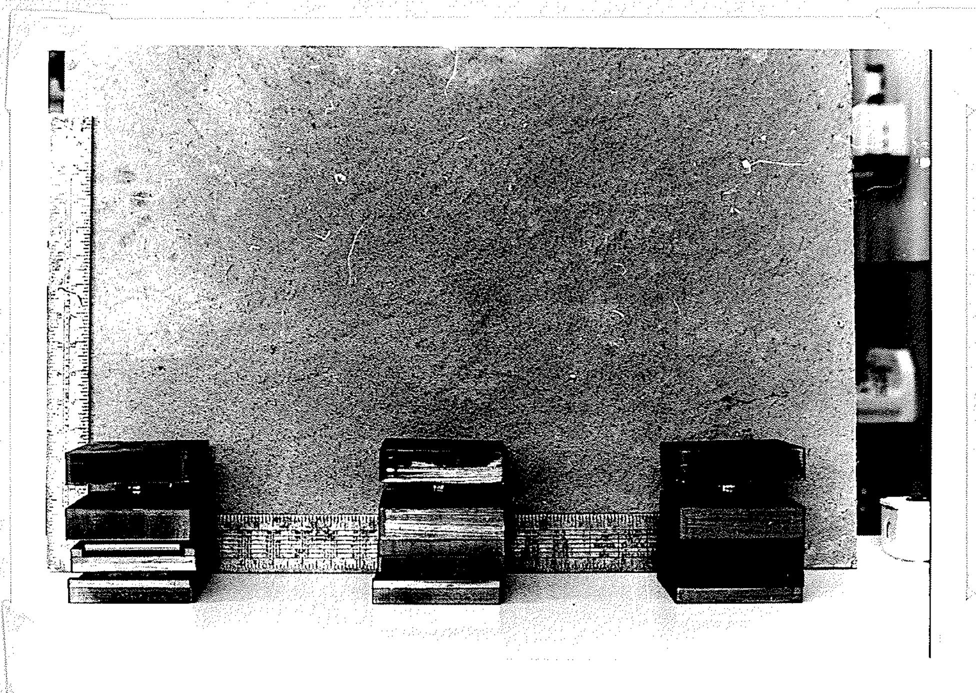

Picture 5

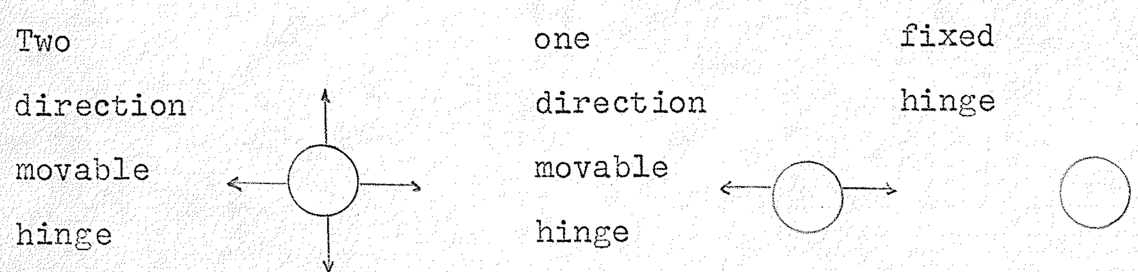

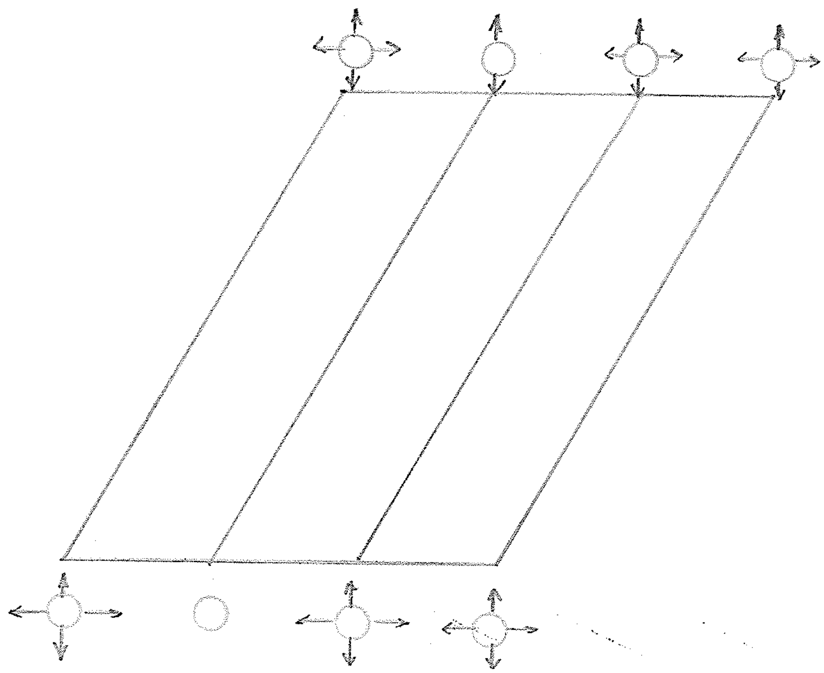

Figure 16

(2) Loading apparatus:

The loading frame consists of two vertical steel columns which were connected by two channels over the test bridge and anchored to two I-beams at the bottom. Concentrated loads were applied to the bridge through two hydraulic jacks which were attached to the channels over the test bridge and a system of load-distributing abutments and supports at the bottom. The hydraulic jacks had a maximum capacity of 3000 psi. The corresponding load capacity was plotted in Figure 17. Several views of the loading apparatus are afforded by Pictures 6 and 7.

(3) Tests: Three tests were carried out by the writer.

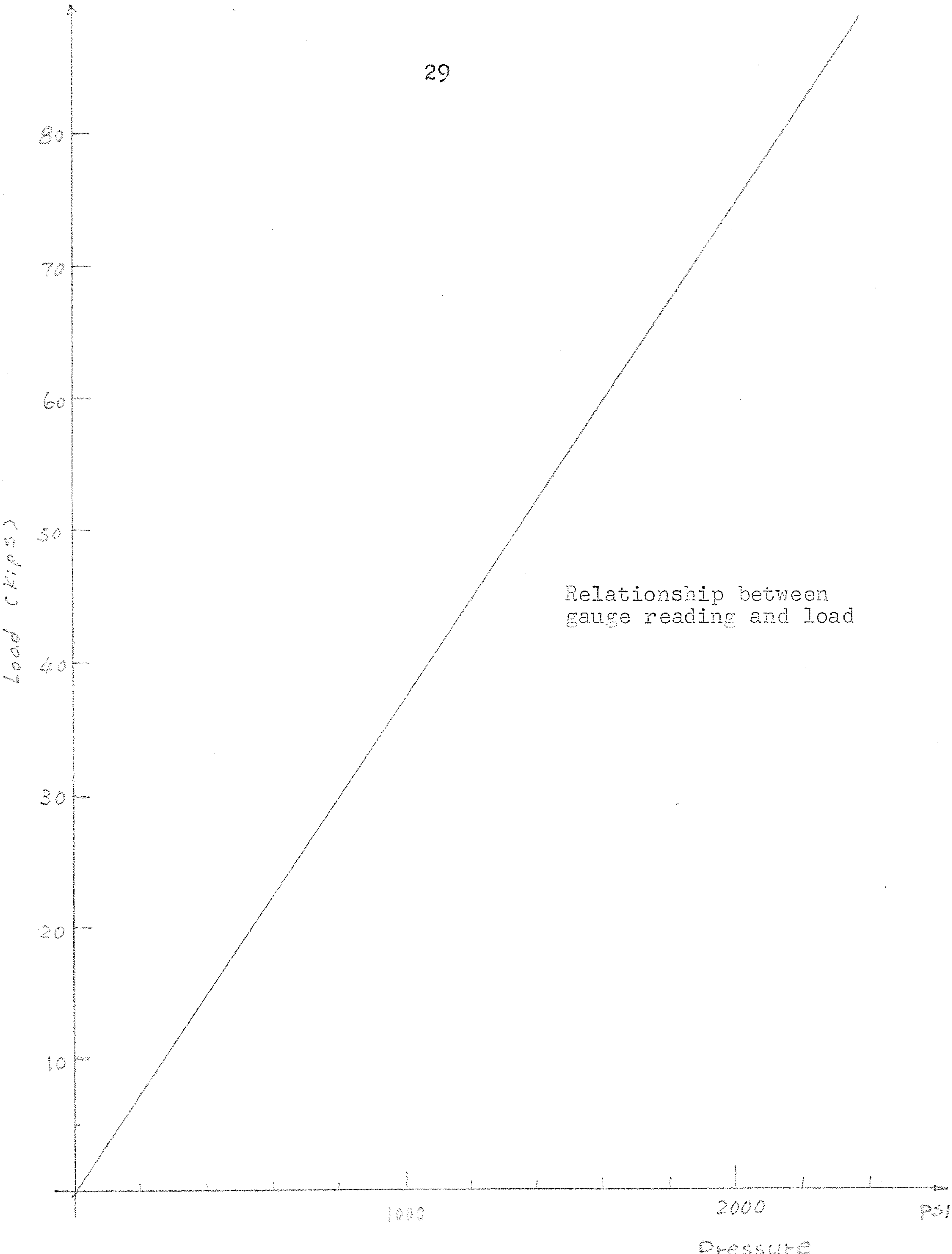
Relationship between
gauge reading and load
Load (Kips)
80
70
60
50
40
30
20
10
1000
2000
PSI
Pressure

Figure 17

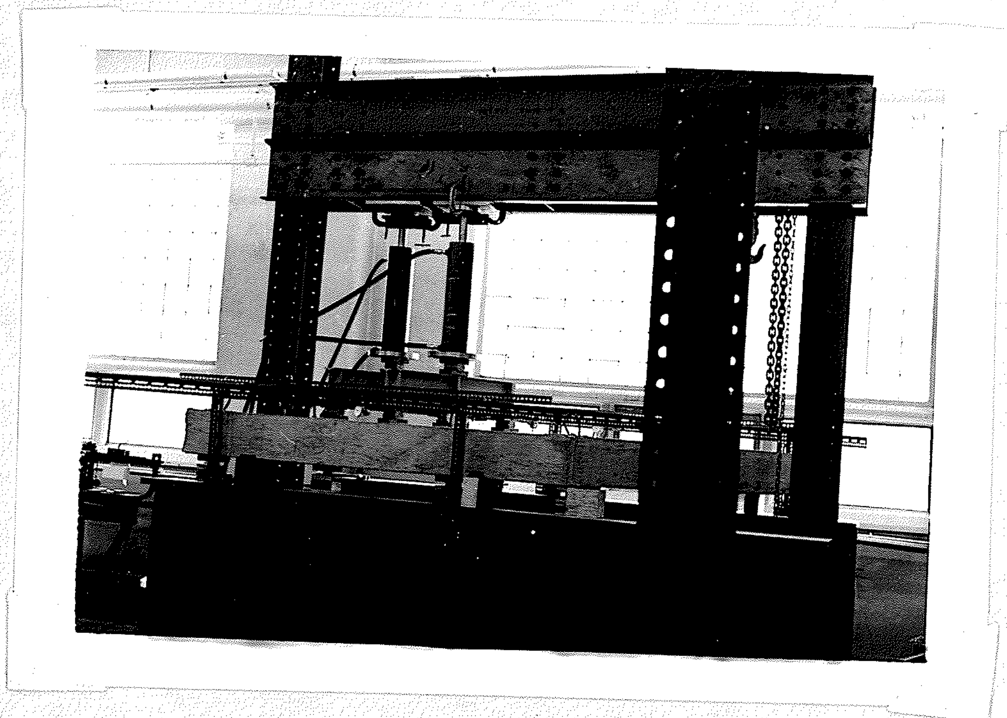

Picture 6

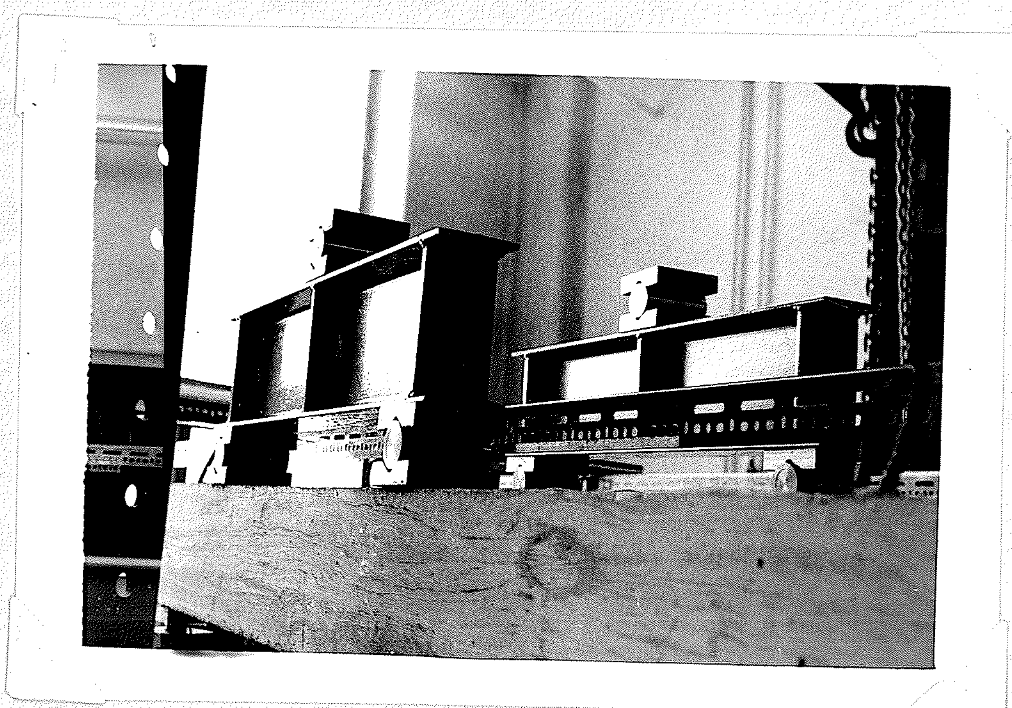

Picture 7

(a). First test: Two pair of loads were applied on the left two beams of bridge No. 1, as shown in Picture 8. The yield line patterns are shown in the left part of Picture 10 and the right part of Picture 11.

(b). Second test: The test was on the same bridge as first test. A pair of loads was placed in the center of the slab of the bridge's undisturbed panel, as shown in Picture 9. The yield line patterns are shown in the right portion of Picture 10 and left portion of Picture 11.

(c). Third test: Two pair of loads were applied on the two internal beams. The bridge was symmetrically cracked as shown in the Pictures 12, 13 and 14.

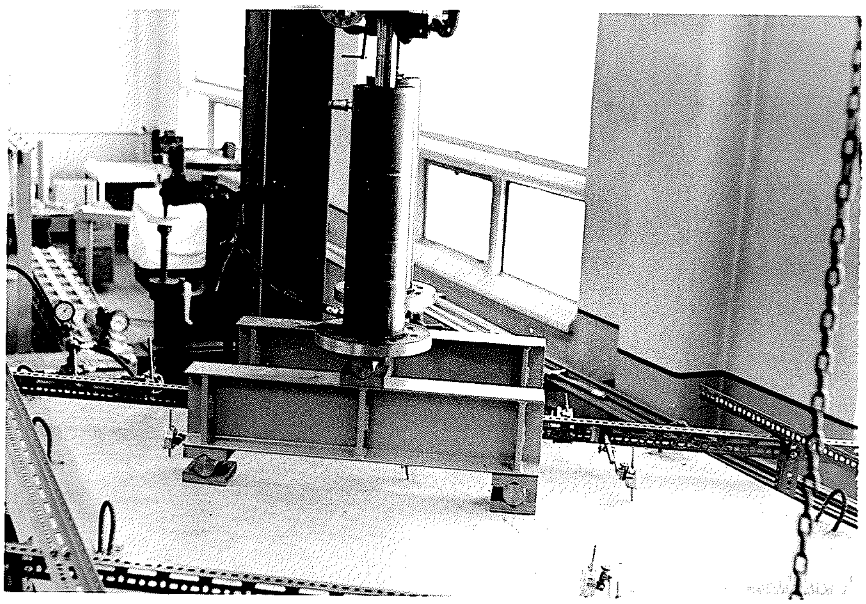

Picture 8

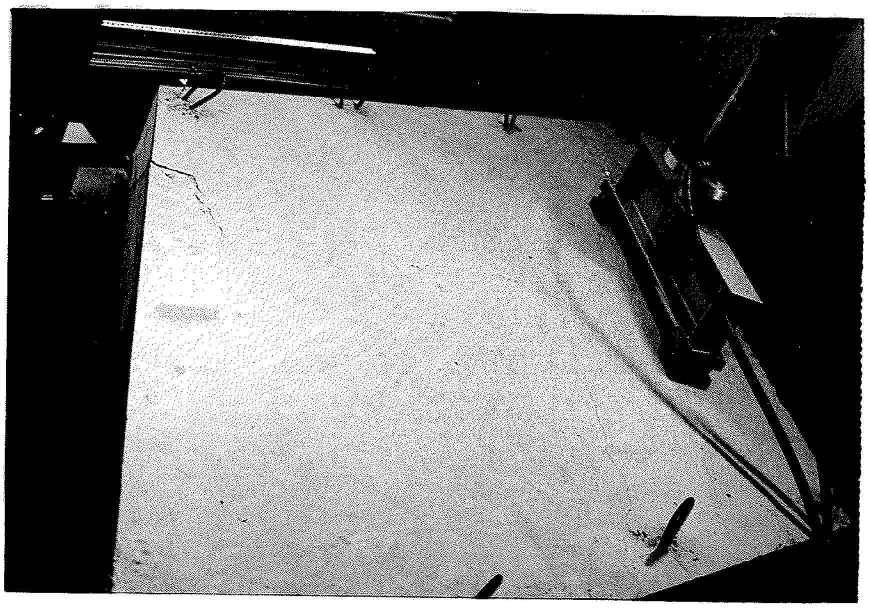

Picture 9

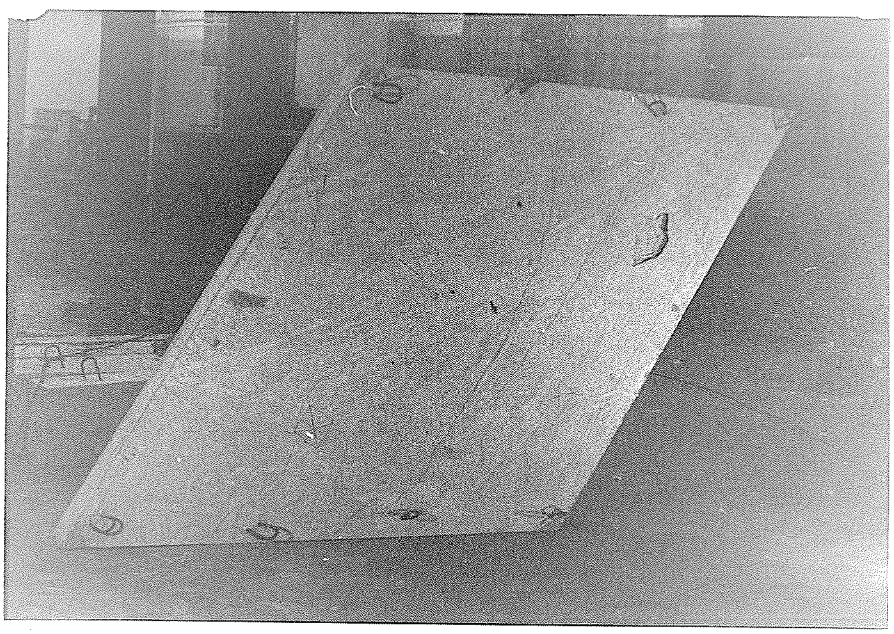

Picture 10

Picture 11

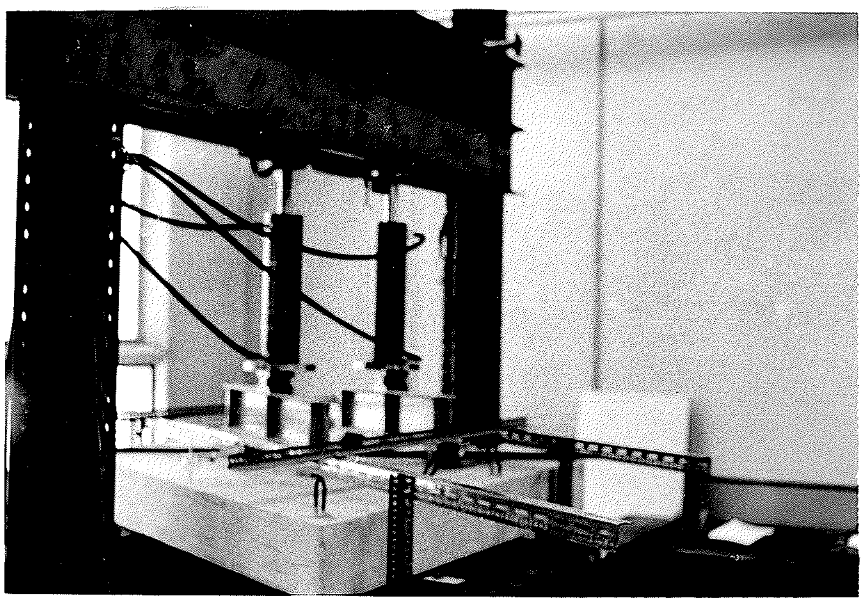

Picture 12

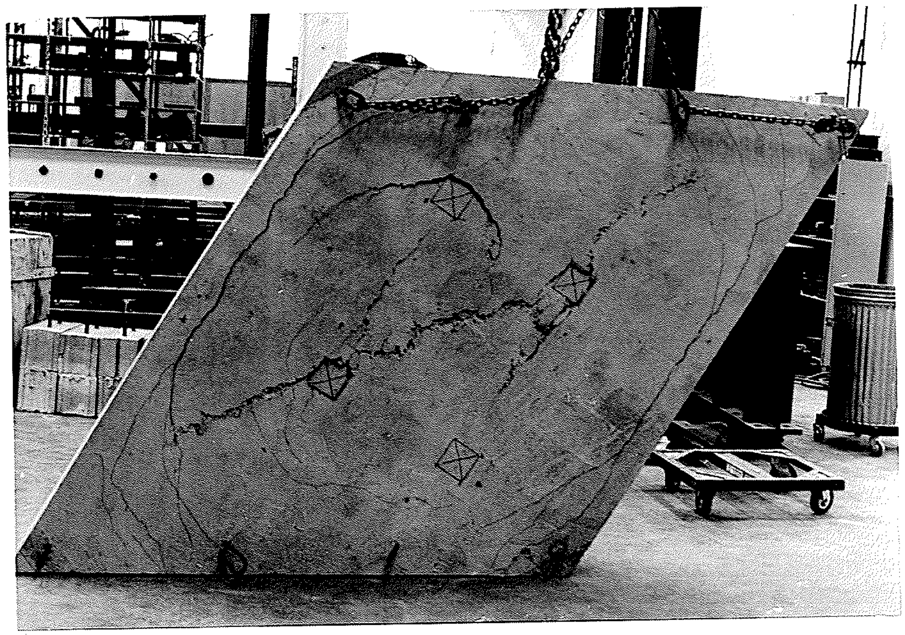

Picture 13

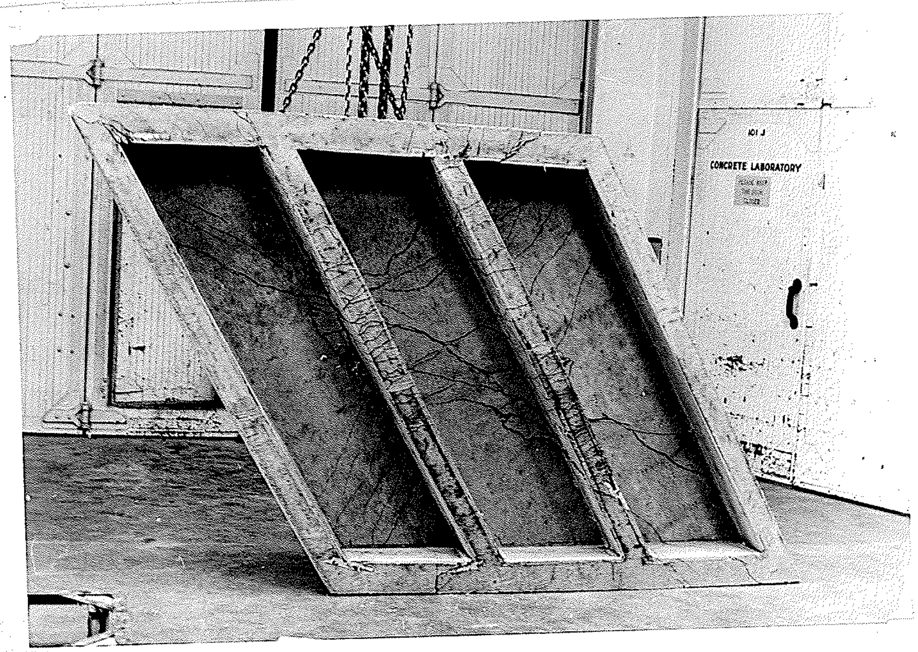

Picture 14

CHAPTER 5

Comparison of theoretical analysis with results of tests.

(1). Property of materials and plastic moments:

Two bridges were built under the same conditions with the same concrete mixture and the same reinforcement except for the transversal beams (see Appendix). The average yield load and stress for the steel are listed in the following table.

Table 2. Property of Steel

	Area (in^2)	Average yield load per bar	Ave. yield stress per bar
$\frac{3}{16}$"	0.028	1867 lb	66700 psi
$\frac{3}{8}$"	0.11	6033 lb	54800 psi
$\frac{1}{2}$"	0.2	9700 lb	48500 psi

The average load per concrete cylinder and average maximum compressive strength of the concrete (f_c') are listed in the following table.

Table 3. Property of Concrete

Days	Average load per specimen (lb)	fc′(psi)
7	153000	5420
28	171000	6070
at time of testing	189700	6720

Referring to Chapter 3, paragraph 4d, the ultimate moment of the slabs and beams for a given amount of reinforcement can be calculated by:

$$M_B = A_S \cdot f_y \cdot (d - \frac{a}{2}) \quad (7)$$

$$M_T = 1.178 \ . \ R \ min. \ Acage \ . \ (K_1 + K_s) \quad (8)$$

The plastic moments of this study are shown in Figure 18 and tabulated in Table 4. For the calculation of plastic moments see Appendix.

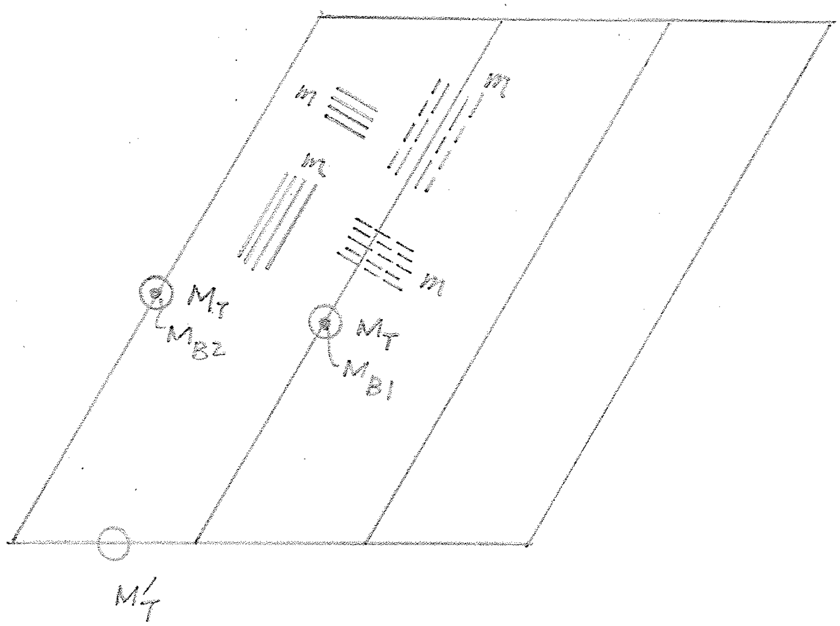

Figure 18

Table 4: Plastic Moments

Moment	Bridge No. 1	Bridge No. 2
m	494 "-lb	
M_B	141000 "-lb	
M	139000 "-lb	
M_T *	15500 "-lb	
M_T '	14300 "-lb	30600 "-lb

Note: $* \; M_T \theta_T = M_T \theta_B \tan 30^\circ = 15500 \times 0.577 \times \theta_B$

$$= 8950 \times \theta_B$$

(2). Basic conception of analysis:

As the structure was gradually loaded to failure, the yielding started from the highly stressed sections and spread into lines dividing the structure to form a definite mechanism system. The prediction of such a collapse mechanism system must be very cautious. Some conditions for prediction of yield line pattern for slabs were given by Jones[7] as follows:

(a). Yield lines end at a slab boundary.

(b). Yield lines are straight.

(c). A yield line, or yield line produced, passes through the intersection of the axes of rotation of adjacent slab elements.

(d). Axes of rotation generally lie along lines of supports and pass over any columns.

These conditions can also be applied to the composite slab and beam structures. In this type of structure a yield line can end at the beams but if yield line crosses the beams a combined torsional and bending hinge is placed at the crossing point.

Usually several families of yield line patterns can often be postulated and the minimum ultimate load examined by using a virtual work equation based on the concept of conservation of energy and can be expressed by:

$$\Sigma(P_u \cdot \delta) = \Sigma(M \cdot \theta)$$

where $\Sigma(P_u \cdot \delta) = \Sigma \iint w \cdot \delta \cdot dx \cdot dy$

= work done due to external loads

$\Sigma(M\theta) = \Sigma(m\,\ell\,\theta)$

= work dissipated due to deformations.

Some examples are given in sections of 3, 4 and 5 of this chapter.

For a given yield line pattern the worst failure mode can be approximately found by differentiating the parameters (α_i) which are used to locate the yield lines. The mathematical expression is as follows:

$$P_u = f(\alpha_i, m) \quad ; \quad \frac{\partial P_u}{\partial \alpha_i} = 0 \quad \cdots\cdots$$

where $i = 1, 2, 3, 4 \ldots\ldots$

A trial method can also be used to find the worst failure mode of a given yield line pattern. Figure 19 shows a one sided free and three sided simply supported slab with a uniformly distributed load (W_u).

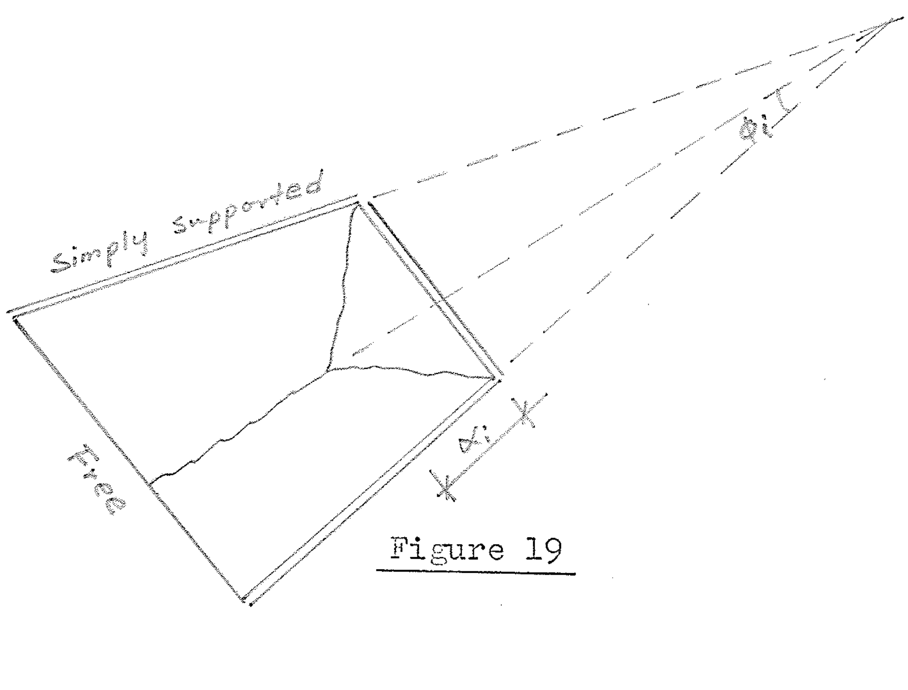

Figure 19

The minimum W_u can be found by a different combination of ϕ_i and α_i, as shown in Table 5.

Table 5. Number of combination of W_u

Number of ϕ_i	Number of α_i 1	2	3	4	.	.	.	.	.
1	1	2	3	4	.	.	.	.	.
2	2	4	6	8	.	.	.	.	.
3	3	6	9	12	.	.	.	.	.
.	.	.	.	.	.	.	.	.	.
.	.	.	.	.	.	.	.	.	.

(3). First analysis:

Bridge No. 1 was assumed to be loaded by four concentrated loads acting on the left two beams. Five failure modes were postulated as shown in the Figures 20, 21, 22, 23 and 24. The corresponding calculations are tabulated as shown in Tables 8, 9, 10, 11 and 12. The critical ultimate load as calculated was 6.55 kips- as shown in Figure 24 and Table 12. The actual critical ultimate load as a result of the test was 10 kips.

(4). Second analysis:

Two concentrated loads were assumed to be applied to the undisturbed panel of bridge No. 1. The predicted yield line patterns and their corresponding analytical values are listed in Table 6. They indicated that the minimum $P_u = 6.22$ kips. The result of the test was a $P_u = 11$ kips.

Table 6

Figure	K	m "-lb	$P_u = Km$	Page
9	16	494	7900	20
10	15	494	7420	20
11	13.28	494	6570	21
12	12.56	494	6220	21
15	18.4	494	9100	22

(5). Third analysis:

Bridge No. 2 was assumed to be loaded by four truck loads acting directly on the two internal beams. Five failure modes were postulated and examined as shown in Figures 25, 26, 27, 28 and 29. and Tables 13, 14, 15, 16 and 17. The analytical minimum ultimate load was calculated to be 10 kips. The result of the test was a $P_u = 14$ kips.

(6). Summary:

A comparison of theoretical analysis with the results is listed in Table 7.

Table 7

Test	cal. P_u	Gauge reading	test P_u	$\frac{\text{test Pu}}{\text{cal. Pu}}$
1	6.55 kips	1100 psi	10 kips	1.53
2	6.22 kips	1200 psi	11 kips	1.77
3	10. kips	1500 psi	14 kips	1.4

TABLE 7 a

Summary of analysis for tests 1 and 3.

FIGURE	P_u (KIPS)
20	12
21	11.2
22	11.0
23	7.3
24	6.55
25	14.75
26	14.25
27	13.75
28	10.8
29	10.0

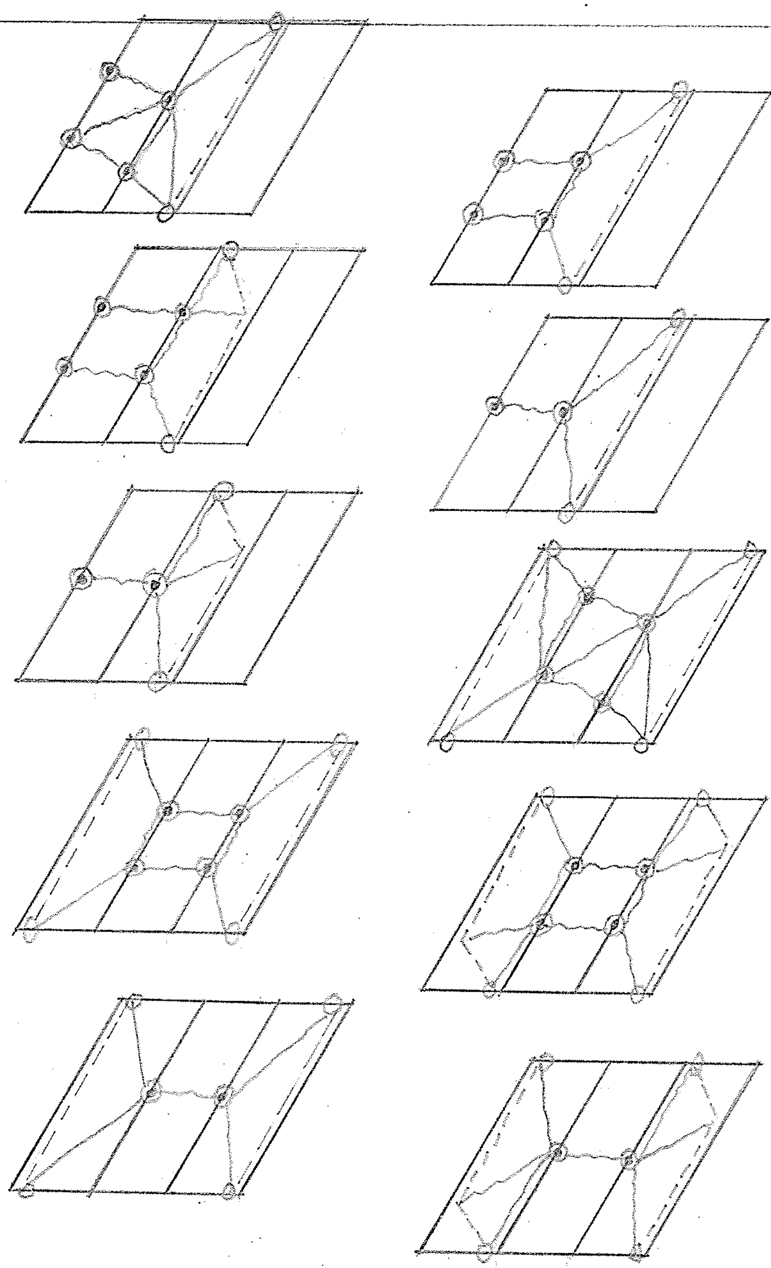

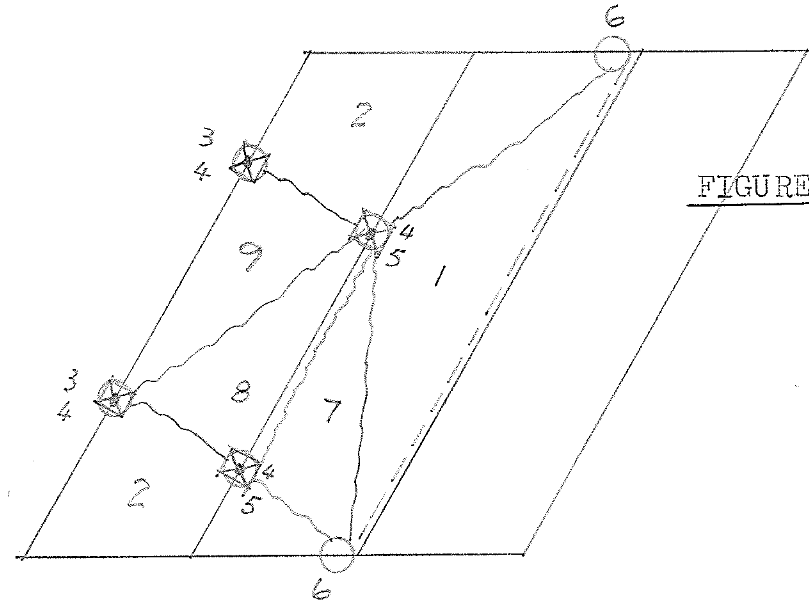

FIGURE 20

TABLE 8

Item	Num.	m "-lb/"	ℓ"	M "-#	θ	Mθ	nMθ
1	2	494	64		$\frac{1}{16}$	1976	3952
2	2	494	36		$\frac{1}{21}$	847	1694
3	2			139000	$\frac{1}{21}$	6620	13240
4	4			8950	$\frac{1}{21}$	426	1700
5	2			141000	$\frac{1}{21}$	6700	13400
6	2			14300	$\frac{1}{21}$	680	1360
7	2	494	34		$\frac{198}{714}\times\frac{1}{14}$	332	664
8	2	494	34		$\frac{9}{21}\times\frac{1}{14}$		
9	1	494	34		$\frac{9}{21}\times\frac{1}{14}$		1660
	1	494	8		$\frac{9}{21}\times\frac{1}{14}$		
							37660 "-lb

$$Pu \times \left(1+1+\frac{12}{21}+\frac{12}{21}\right) = 37660 \text{ "-\#}$$

$$Pu = \frac{37660}{3.15} = \underline{\underline{12000\#}}$$

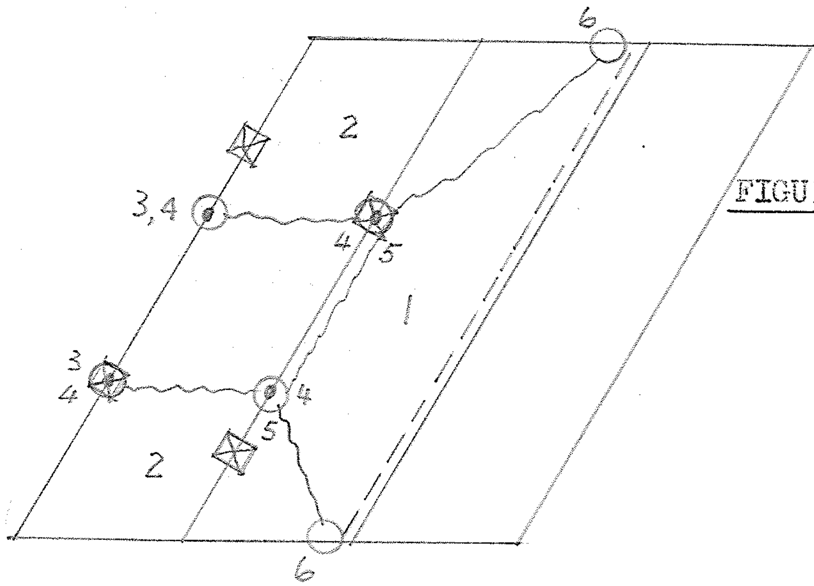

FIGURE 21

TABLE 9

Item	Num.	m "-#/"	ℓ "	M "-#	θ	Mθ	nMθ
1	2	494	64		$\frac{1}{16}$	1976	3952
2	2	494	36		$\frac{1}{21}$	847	1694
3	2			139000	$\frac{1}{21}$	6620	13240
4	4			8950	$\frac{1}{21}$	426	1700
5	2			141000	$\frac{1}{21}$	6700	13400
6	2			14300	$\frac{1}{21}$	680	1360
							35346 "-#

$$P_u \times \left(1+1+2\,\frac{12}{21}\right) = 35346 \text{ "-\#}$$

$$P_u = \frac{35346}{3.15} = \underline{\underline{11200\#}}$$

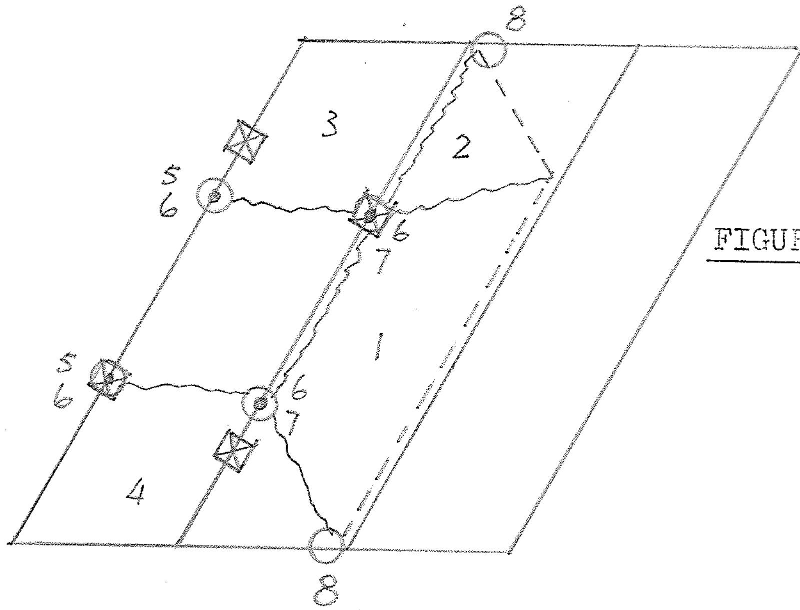

FIGURE 22

TABLE 10

Item	Num.	$m''^{-\#}/''$	ℓ''	$M''^{-\#}$	θ	$M\theta$	$nM\theta$
1	2	494	46		$\frac{1}{16}$	1420	2840
2	2	494	18		$\frac{1}{20}$	444	888
3	1	494	18		$\frac{1}{21}$	444	444
4	1	494	36		$\frac{1}{21}$	888	888
5	2			139000	$\frac{1}{21}$	6620	13240
6	4			8950	$\frac{1}{21}$	426	1700
7	2			141000	$\frac{1}{21}$	6700	13400
8	2			14300	$\frac{1}{21}$	680	1360
							$34760\ ''^{-\#}$

$$Pu = \frac{34760}{3.15} = \underline{\underline{11000\#}}$$

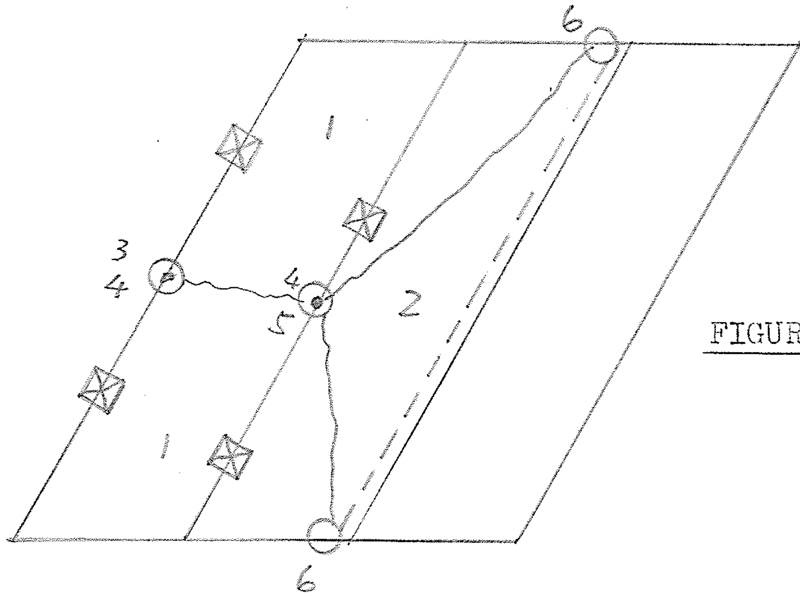

FIGURE 23

TABLE 11

Item	Num.	m ″-#/″	ℓ″	M ″-#	θ	Mθ	nMθ
1	2	494	36″		$\frac{1}{30}$		1185
2	2	494	64″		$\frac{1}{16}$	1975	3950
3	1			139000	$\frac{1}{30}$		
4	2			8950	$\frac{1}{30}$	$\frac{326500}{30}$ =	10900
5	1			141000	$\frac{1}{30}$		
6	2			14300	$\frac{1}{30}$		

16035 ″-#

$$Pu \times \left(\frac{21}{30} + \frac{21}{30} + \frac{12}{30} + \frac{12}{30}\right) = 16035 \text{ ″-\#}$$

$$Pu = \frac{30}{66} \times 16035 = \underline{\underline{7300\#}}$$

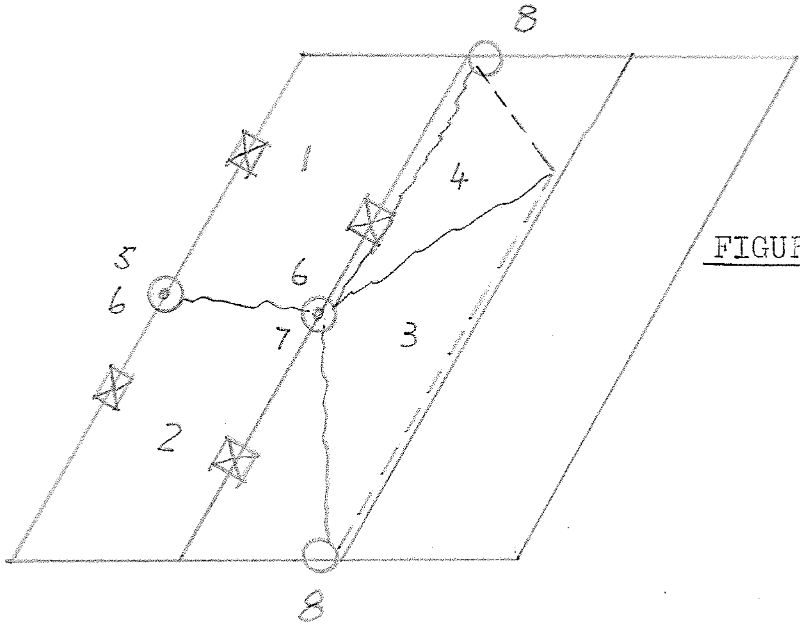

FIGURE 24

TABLE 12

Item	Num	m ''-#/''	ℓ''	M ''-#	θ	$M\theta$	$nM\theta$
1	1	494	18		$\frac{1}{30}$	296	296
2	1	494	36		$\frac{1}{30}$	592	592
3	2	494	46		$\frac{1}{16}$		2840
4	2	494	18		$\frac{1}{30}$	296	592
5	1			139000	$\frac{1}{30}$	4630	4630
6	2			8950	$\frac{1}{30}$	298	596
7	1			141000	$\frac{1}{30}$	4700	4700
8	2			14300	$\frac{1}{30}$	477	954
							14400 ''-#

$$Pu = \frac{30}{66} \times 14400 = \underline{\underline{6550\#}}$$

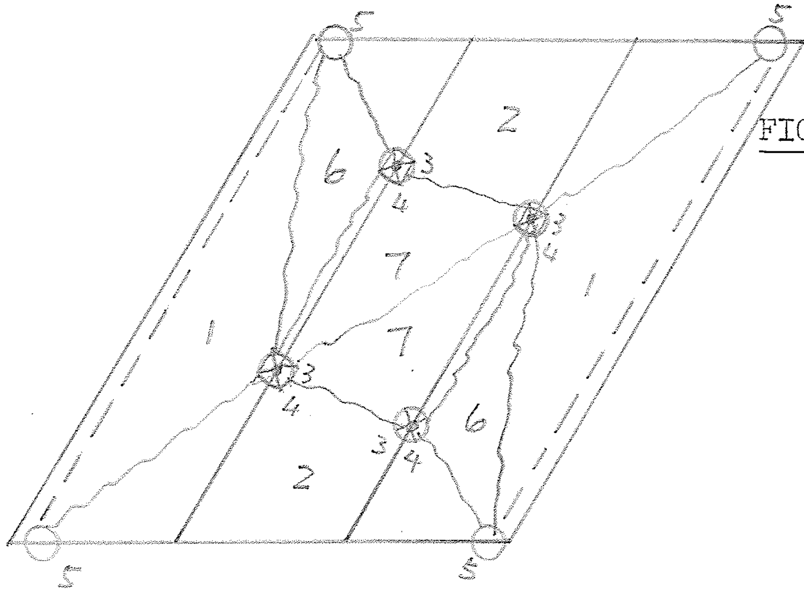

FIGURE 25

TABLE 13

Item	Num.	m"-#/"	ℓ"	M"-#	θ	M θ	nMθ
1	4	474	64		$\frac{1}{16}$	1976	7900
2	2	474	54		$\frac{1}{21}$	1270	2540
3	4			141000	$\frac{1}{21}$	6720	26800
4	4			8950	$\frac{1}{21}$	4260	1700
5	4			30600	$\frac{1}{21}$	1460	5830
6	4	474	34		$\frac{198}{714} \times \frac{1}{14}$	331	1324
7	4	474	34		$\frac{3}{7} \times \frac{1}{14}$	513	2050

46144 "-#

$$Pu = \frac{46144}{3.15} = \underline{\underline{14.75}} \text{ kips}$$

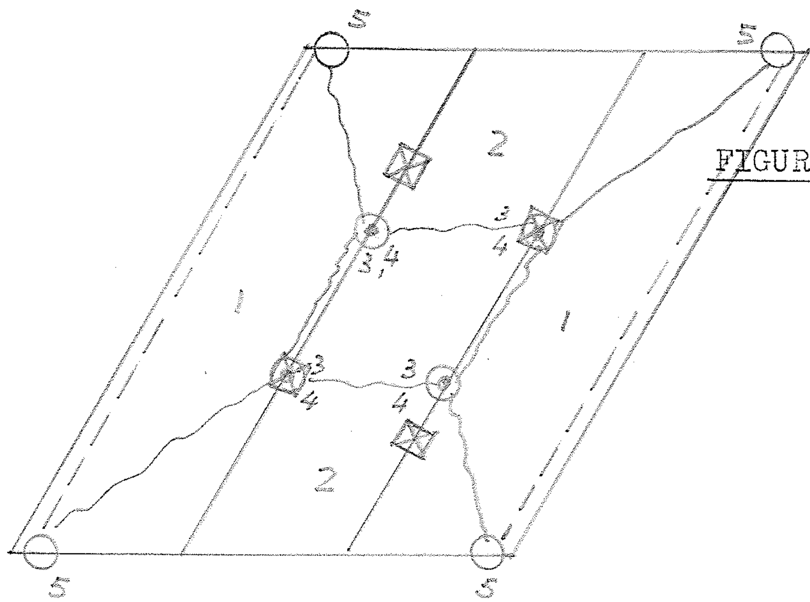

FIGURE 26

TABLE 14

Item	Num.	m"-#/"	l"	M"-#	θ	Mθ	nMθ
1	4	494	64		$\frac{1}{16}$	1976	7900
2	2	494	54		$\frac{1}{21}$	1270	2540
3	4			141000	$\frac{1}{21}$	6720	26900
4	4			8950	$\frac{1}{21}$	426	1700
5	4			30600	$\frac{1}{21}$	1455	5820
							44860"-#

$$P_u = \frac{44860}{3.15} = \underline{\underline{14.25}} \text{ kips}$$

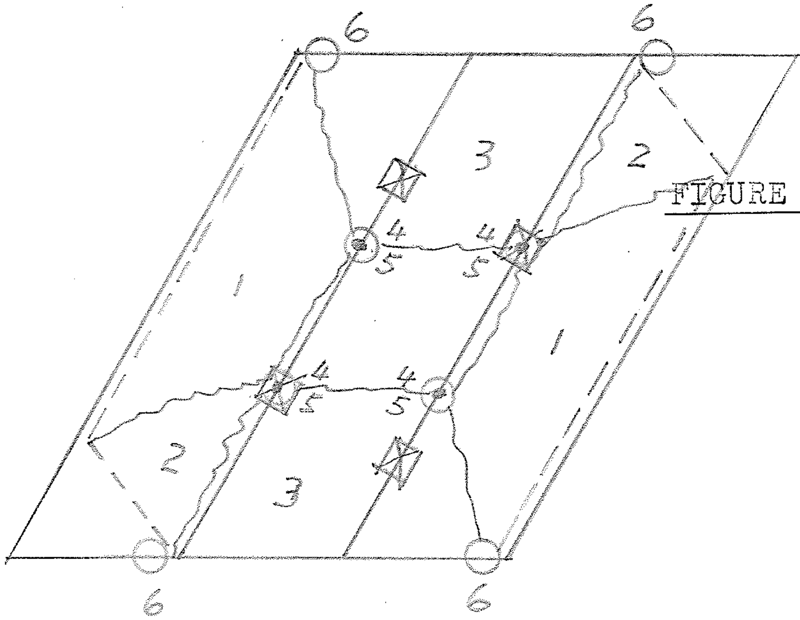

FIGURE 27

TABLE 15

Item	Num	m "-#/"	ℓ"	M "-#	θ	Mθ	nMθ
1	4	494	46		$\frac{1}{16}$	1420	5680
2	4	494	16		$\frac{1}{20}$	395	1580
3	2	494	36		$\frac{1}{21}$	846	1690
4	4			141000	$\frac{1}{21}$	6720	26900
5	4			8950	$\frac{1}{21}$	426	1700
6	4			30600	$\frac{1}{21}$	1455	5820

43370 "-#

$$Pu = \frac{43370}{3.15} = \underline{\underline{13.75}} \text{ kips.}$$

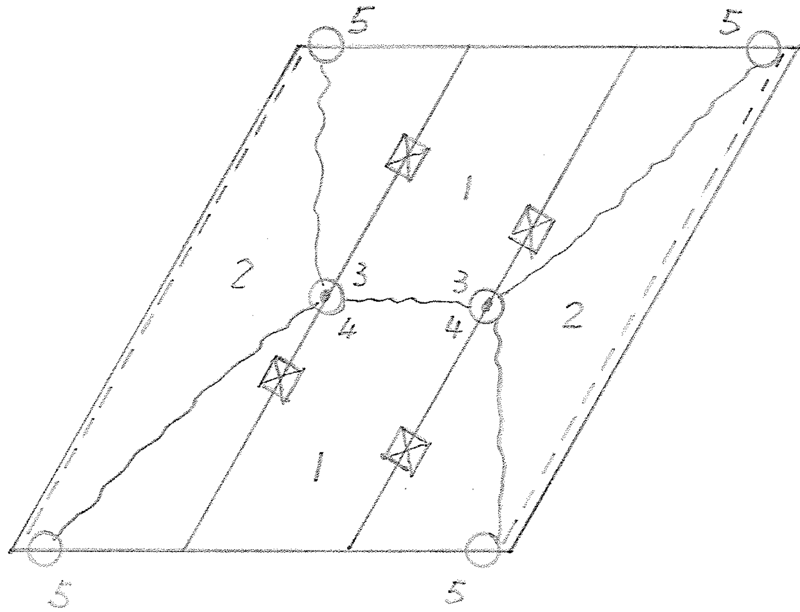

FIGURE 28

TABLE 16

Item	Num.	m ''-#/''	ℓ''	M ''-#	θ	Mθ	nMθ
1	2	494	54		$\frac{1}{30}$	890	1780
2	4	494	64		$\frac{1}{16}$	1975	7900
3	2			141000	$\frac{1}{30}$		9400
4	2			8950	$\frac{1}{30}$		598
5	4			30600	$\frac{1}{30}$		4080

23758 ''-#

$$Pu = \frac{30}{66} \times 23758 = \underline{\underline{10.8}} \text{ kips}$$

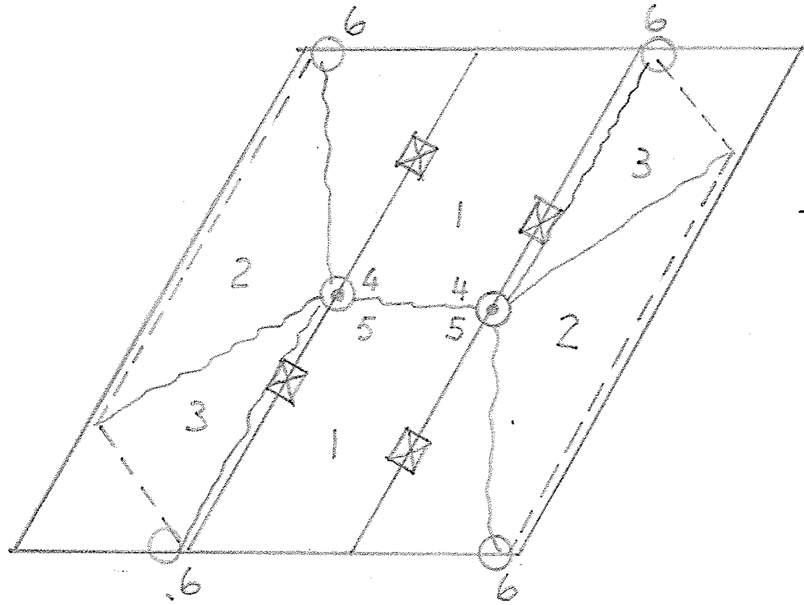

FIGURE 29

TABLE 17

Item	Num	$m^{''-\#/''}$	ℓ''	$M^{''-\#}$	θ	$M\theta$	$nM\theta$
1	2	494	36		$\frac{1}{30}$	592	1184
2	4	494	46		$\frac{1}{16}$		5680
3	4	494	18		$\frac{1}{30}$	296	1184
4	2			141000	$\frac{1}{30}$		9400
5	2			8950	$\frac{1}{30}$		598
6	4			30600	$\frac{1}{30}$		4080
							22126 $''-\#$

$$Pu = \frac{30}{66} \times 22126 = \underline{\underline{10.}} \text{ kips}$$

CHAPTER 6

DISCUSSIONS AND CONCLUSIONS

(1). Discussion of tests:

Dial gauges were used to measure the deflections of the bridge. The gauges could measure a maximum deflection of one inch, however, the maximum deflection reached two inches. In addition, the movement of the bridges - Picture 15 and the twisting of gauge frame - Picture 16 made the gauge readings useless. A possible improvement is to reduce the degree of freedom of the bridges, as shown in Figure 30. In order to increase the rigidity of the

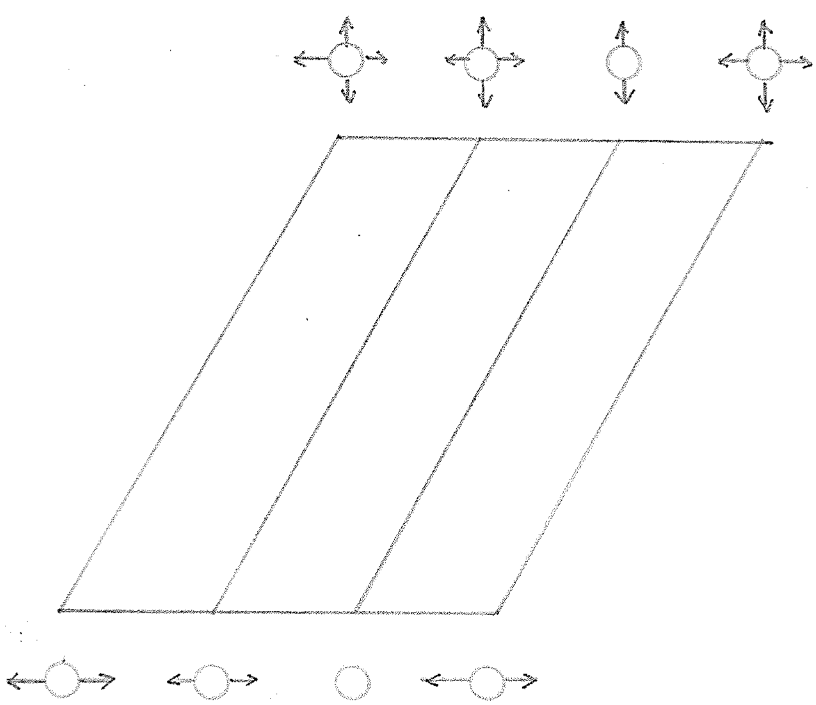

Figure 30

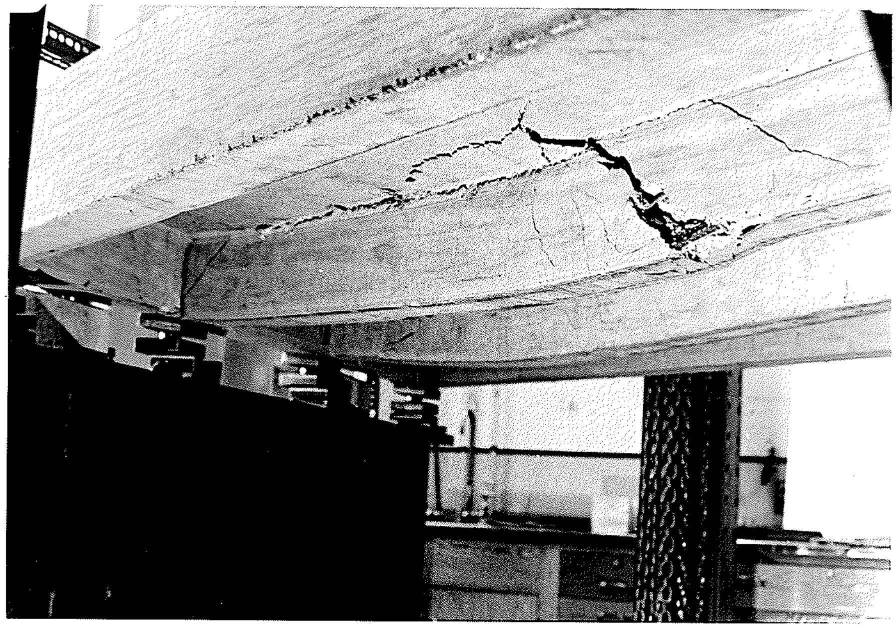

Picture 15

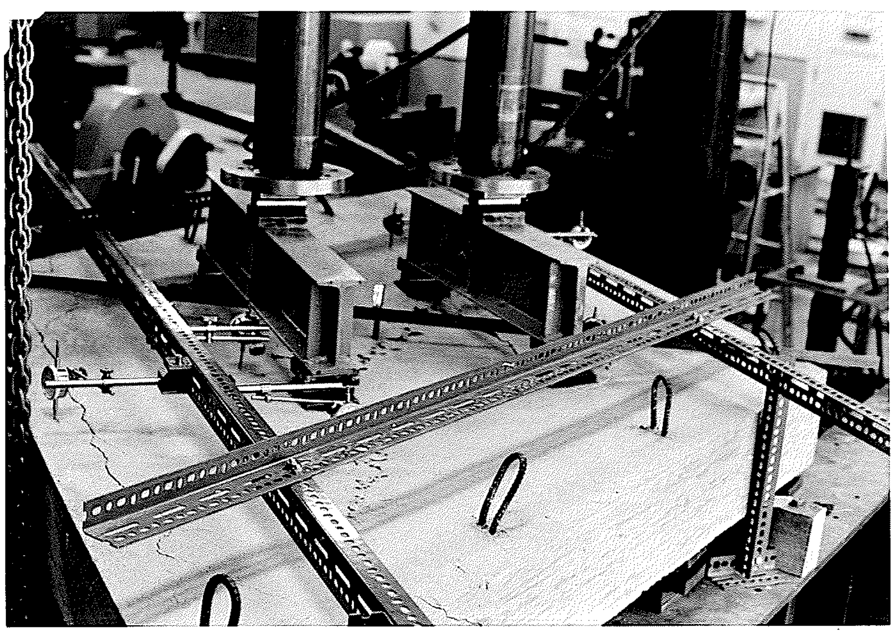

Picture 16

gauge frame, a steel frame should be used instead of dexion.

Owing to the elastic assumption that the negative moment of continuous slabs takes place over the support and the positive moment occurs at the middle of the span, the conventional construction of bottom reinforcement usually means that it is lapped at the support as shown in Figure 31.

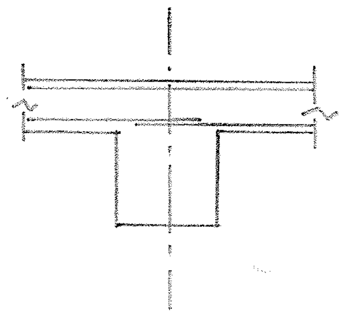

Figure 31

This is not sufficient, as the writer's tests showed that the sagging yield line could also occur when certain heavy loads acted upon the beams (Picture 15). Therefore, enough anchorage length of bottom steel at the support should be considered for some cases.

As a result of the tests it was found that the ultimate loads were much larger than those predicted in Table 7. This phenomenon indicated the presence of membrane action[11] which decreased the yielding moment with tensile in-plane forces and increased the yielding moment with compressive in-plane forces. The relationship between overall forces (P-compression, T-tension) with its corresponding moments (M) and the full plastic moment (M_o) with its corresponding force ($T_o = A_s \cdot f_y$) can be expressed by

$$\frac{M}{M_o} = 1 + \alpha \cdot \frac{P}{T_o} - \beta \left(\frac{P}{T_o}\right)^2$$

where $\alpha = \dfrac{\frac{1}{2}\frac{d}{d_1} - \frac{3}{2}t}{1 - \frac{3}{4}t}$; $\beta = \dfrac{\frac{3}{4}t}{1 - \frac{3}{4}t}$

$t = \dfrac{A_s}{d_1} \cdot \dfrac{0.78 f_y}{f_c'}$

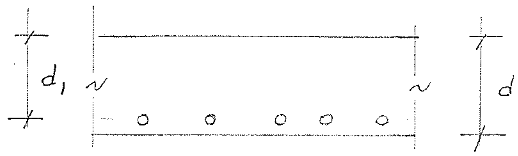

d = thickness

d_1 = depth of slab

This equation can be plotted as shown in Figure 32 and gives the maximum and minimum values as follows:

$M_{max} = (1 + \frac{\alpha^2}{4\beta}) M_o$

$M_{min} = (1 - \alpha - \beta) M_o$

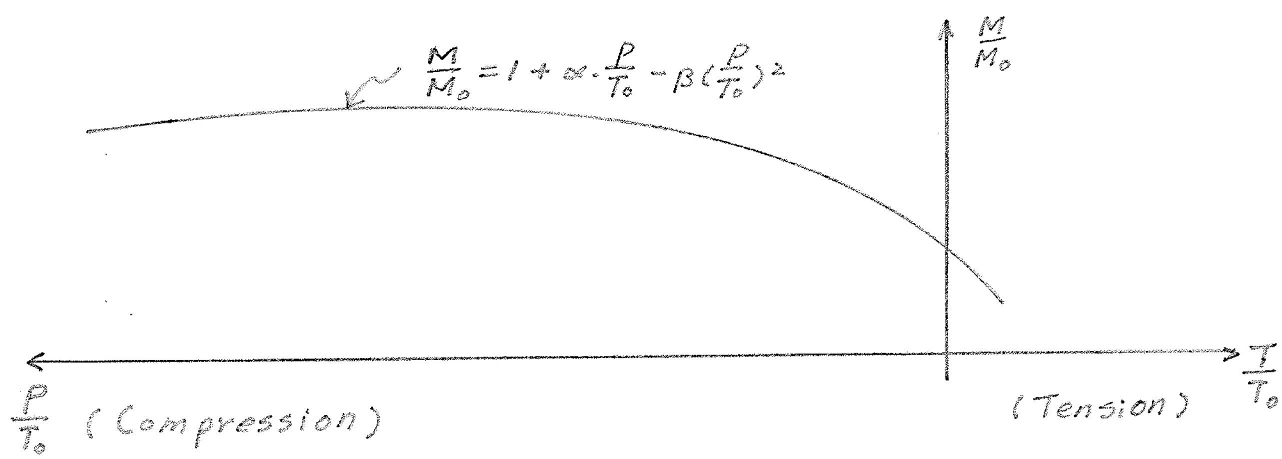

Figure 32

In the first test, the ratio of test result to the predicted load was 1.53. It is clear that the compressive membrane action, as demonstrated above, increased the carrying capacity until a second shear failure took place as shown in Picture 17.

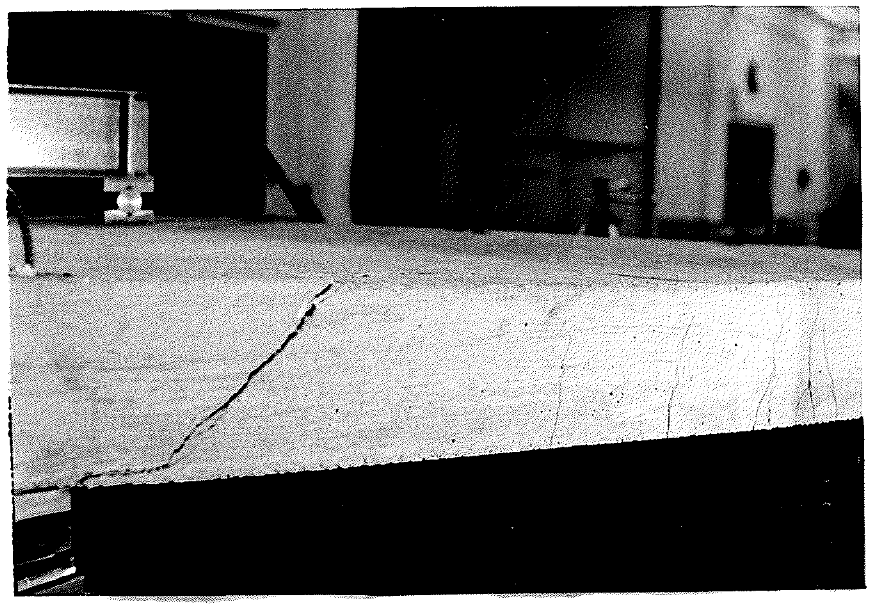

Picture 17

In the second test, the predicted yield line pattern was a circular fan (Figure 12) with an ultimate load of 6.22 kips. Because of compressive membrane action, the predicted pattern could not be formed but switched to the easier type of Figure 15. This was still under membrane action until the pun~~t~~ching sh ear failure took place with a final maximum load of 11 kips.

In the third test, the maximum load attained during the test was 14 kips.--about 40 percent greater than predicted. This also indicated that the compressive membrane action was present until the internal beams failed in shear.

(2). Conclusions:

From this study it may be concluded that the method of combined yield lines and yield hinges used to solve reinforced concrete slab and beam structures is valid, safe and economical if the load factor remains at the same level as in elastic design.

The current ultimate design is restricted to designing sections only. The factored moments and shears, which this design is based on, are still determined by using elastic theory. This combination of design could be considered contradictory. The success of the yield line and yield hinge method makes the ultimate design rational.

The concept of virtual work being applied to this method is very easy to understand and simple to apply. For irregular or complicated structures either the elastic solution is very laborious or an elastic solution is as yet impossible. The method of combined yield lines and yield hinges makes all solutions of such structures short, simple and sound in theory.

(3). Limitations and future research work:

In applying the yield line and yield hinge method to structures, some limitations which arise either from the properties of materials or from severe types of loads applied to the structures must be borne in mind by the analyst.

The occurrence of membrane action in the tests causes the analysis to be inaccurate. To utilize this action in design problem further research is necessary. (11)

In comparing other test results of membrane action with the writer's tests, it was shown that owing to the occurrence of shear failure, the membrane action in the writer's tests could not be fully developed. The problem of shear is still not fully solved. The research of flexural shear in beams is going on at the University of Toronto and elsewhere. Also a study of ultimate shear strength will start in the near future in the University of Manitoba.

The brittle fracture lines, due to the lack of ductility of concrete, are always confused with plastic yield lines. The study of ductility of reinforced concrete is also on the list of future research at the University of Manitoba.

BIBLIOGRAPHY

1. Koch, W. "Brückenbau" Teil 3. Düsseldorf, Werner-Verlay, 1962.

2. Newmark, N.M., Siess, C.P., Peckham, W.M. "Studies of slab and beam highway bridges--Part II, Tests of simple-span skew I-beam bridges." Bulletin No. 375 University of Illinois, Eng. Expt. Sta. Jan. 1948.

3. Chen, T.Y., Siess, C.P., Newmark, N.M. "Studies of slab and beam highway bridges, Part VI. Moments in simply supported skew I-beam bridges." Bulletin No. 439. University of Illinois, Eng. Expt. Sta. Jan. 1957.

4. Mörsch, E., "Brücken aus Stahlbeton und Spannbeton". Stuttgart Verlag Konrad Wittner, 1958.

5. Rowe, R.E., "Concerte Bridge Design." John Willey & Sons Inc., 1962.

6. Taylor, W., Thompson, S.E., Smulski, E., "Reinforced-concrete Bridges". John Willey & Sons, 1939.

7. Jones, L.L. "Ultimate Load Analysis of Reinforced and Prestressed Concrete Structures." Chatto and Windus Ltd., London, 1962.

8. Lansdown, A.M. "An Investigation into the Ultimate Behaviour of Reinforced Concrete Beam and slab structures, in particular Bridge Deckes." Ph. D. Thesis. 1964.

9. Mattock, A.H. "Structural Model Testing-Theory and Application." Journal of the PCA Research & Development Lab. Bulletin D56 Vol. 4, No. 3, 12-23. Sept. 1962.

10. AASHO. "The American Association of State Highway Officials.--Standard Specifications for Highway Bridges." 1957.

11. Wood, R.H. "Plastic and Elastic Design of Slabs and Plates." London, Thames and Hudson, 1961.

APPENDIX

CALCULATION OF PLASTIC MOMENTS

(1). Moment of slab:

$f_c' = 6720$ psi

$fy = 66700$ psi

$u = \frac{fc'}{0.78} = 8630$ psi

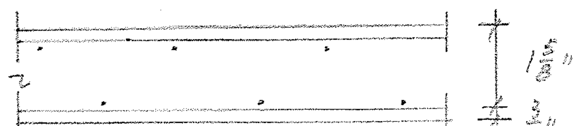

$\frac{3}{16}"\phi$ @ 6" Both Way

$\alpha u = 4250$ psi

use $\frac{3}{16}"\phi$ @ 6" $A_s = 0.056\ in^2$ both way

$A_s \cdot fy = 0.056 \times 66700 = 3730$ #/,

$d = 2 - \frac{3}{8}" = \frac{15}{8}" = 1.625"$

$a = \frac{3730}{12 \times 4250} = 0.078"$

$(d - \frac{a}{2}) = 1.625 - 0.0365 = 1.588 \doteq 1.59"$

$m = 1.59 \times 3730 = 5930" - \#/, = \underline{\underline{494" - \#/"}}$

(2). Moment of longitudinal beams:

M_{B1} = Bending moment of internal beams

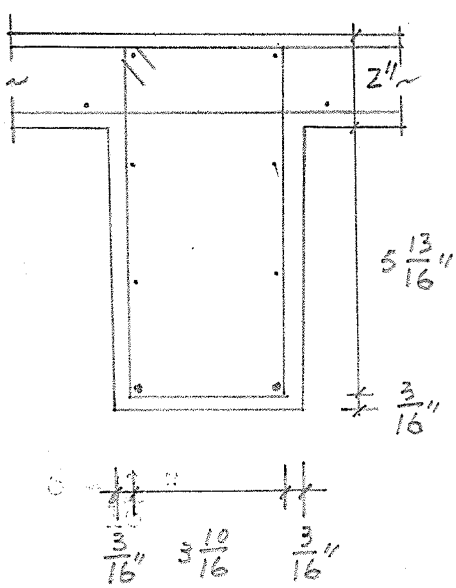

$6 - \frac{3}{16}"\phi$

2 - #4 $A_s = 0.4$

$d = 8 - \frac{3}{8}" - 0.25" = 7.375"$

$A_s fy = 0.4 \times 48500 = 19400$ #

$b\,\alpha\,u = 20 \times 4250 = 85000$

$a = \frac{19.4}{85} = 0.228$

$d - \frac{a}{2} = 7.261"$

$M_{B1} = 7.261 \times 19400 = \underline{\underline{141,000" - \#}}$

2 - #4 ($f_y = 48500$ psi)

stirrups $\frac{3}{16}$" ϕ @ 5"

M_{B2} = Bending moment of external beams

$$b \propto u = 12 \times 4250 = 51000$$

$$a = \frac{19.4}{51} = 0.38$$

$$d - \frac{a}{2} = 7.185''$$

$$M_{B2} = 7.185 \times 19400 = \underline{\underline{139,000}}\ ''\text{-}\#$$

M_T = torsional moment of longitudinal beams

$$6 - \frac{3}{16}''\ \phi \qquad A_s = 0.168\ in^2$$

$$A_s f_y = 0.168 \times 66700 = 11200\ \#$$

$$d' = 8 - \frac{3}{16} - \frac{3}{16} - \frac{3}{16} = 8 - 0.562 = 7.438''$$

$$b' = 4 - 0.562 = 3.438''$$

$$A_{cage} = b' \times d' = 25.6\ in^2$$

$$c = 2\ (d' + b') = 21.752'$$

$$R_L = \frac{11200}{21.75} = 515 \quad \left(\frac{n\ F_{yc}}{c}\right)$$

$$\frac{F_{yT}}{P} = \frac{2 \times 0.028 \times 66700}{5} = 0.0112 \times 66700$$
$$= 747$$

$$R_{min} = 515$$

$$M_T = 1.178 \times 515 \times 25.6 \times 1 = \underline{\underline{15500}}\ ''\text{-}\#$$

(3). Torsional moment of transversal beams:

Bridge No. 1.

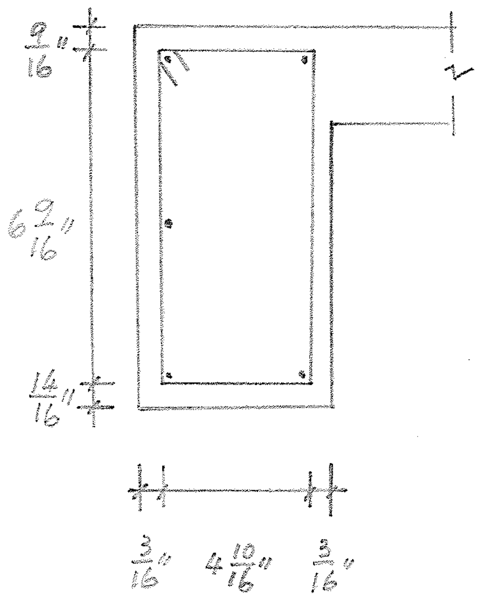

$$d' = 8 - \frac{9}{16} - \frac{14}{16} - \frac{3}{16} = 8 - \frac{13}{8} = 6.375''$$

$$b' = 5 - 0.56 = 4.44''$$

$$Acage = b' \times d' = 28.3 \text{ in}^2$$

$$c = 2(b' + d') = 21.63''$$

$$5 - \frac{3}{16}''\phi \quad A_s = 0.14 \text{ in}^2$$

$$A_s f_y = 0.14 \times 66700 = 9340\#$$

$$R_{min} = \frac{9340}{21.63} = 431$$

$$M_T = 1.178 \times 28.3 \times 431$$

$$= \underline{\underline{14300}} \text{ ''-\#}$$

Bridge No. 2

$d' = 6.375''$

$b' = 4.44''$

$A_{cage} = 28.3\ in^2$

$C = 21.63''$

$4 - \frac{3}{16}''\phi \quad A_s = 0.112\ in^2 \qquad A_s f_y = 0.112 \times 66700 = 7470\ \#$

$2 - \frac{3}{8}''\phi \quad A_s = 0.22\ in^2 \qquad \underline{A_s f_y = 0.22 \times 54800 = 12050}\ \#$

$\Sigma A_s f_y = 19520\ \#$

$$R_{min} = \frac{19520}{21.63} = 920$$

$$M_T = 1.178 \times 920 \times 28.3 = \underline{30600}''\text{-}\#$$